Technical Report

TR-99-29

Processes and features affecting the near field hydrochemistry

Groundwater-bentonite interaction

Jordi Bruno, David Arcos, Lara Duro
QuantiSci

December 1999

Svensk Kärnbränslehantering AB
Swedish Nuclear Fuel
and Waste Management Co
Box 5864
102 40 Stockholm
Tel 08-459 84 00
Fax 08-661 57 19

SKB

Processes and features affecting the near field hydrochemistry

Groundwater-bentonite interaction

Jordi Bruno, David Arcos, Lara Duro
QuantiSci

December 1999

Abstract

This report discusses in a quantitative manner the evolution of the near field aqueous chemistry as a result of the interactions between three different intruding groundwaters (Äspö, Gideå and Finnsjön) with the MX-80 bentonite buffer material.

The main emphasis has been placed on studying the evolution of the main chemical buffers of the system (alkalinity and redox capacities) and the resulting master variables (pH and pe).

The calculations have been done by using a set of thermodynamic and kinetic parameters previously calibrated against experimental data on bentonite/granitic groundwater interactions, in combination with the PHREEQC geochemical code.

The results of the calculations indicate that the alkalinity buffer capacity is mainly exerted by the accessory content of carbonate minerals (calcite) in the bentonite system, while the ion exchange process plays a secondary (but not negligible) role. The Ca(II) content of the intruding groundwater has an impact on the resulting pH. For Ca(II) rich waters, like Äspö, the resulting pH remains in the range of granitic groundwaters (7.5-9.5) during the overall repository lifetime (1 million years). For Ca(II) poor groundwaters, the systems evolves to high alkalinity (pH : 10.5- 10.8) due to the depletion of calcite and the release of carbonate in to the near field aqueous chemistry.

Concerning the reducing capacity of the system, this is mainly controlled by the accessory pyrite content, although the Fe(II) content in montmorillonite and in the carbonates cannot be disregarded. Reducing conditions in the bentonite/groundwater system are ensured throughout the lifetime of the repository system unless this is placed in direct and lifetime contact with the atmosphere (surface storage).

Sammanfattning

Den här rapporten beskriver kvantitativt utvecklingen av närområdets vattenkemi, som en funktion av interaktionerna mellan inträngande grundvatten (Äspö, Finnsjön och Gideå) och buffertmaterialet.

Tonvikten har lagts på studier av de viktiga kemiska buffertarna (alkalinitet och redox kapacitet) och utvecklingen av de resulterande variablerna (pH och pe).

Beräkningarna har gjorts med det geokemiska beräkningsprogrammet PHREEQC, tillsammans med en uppsättning termodynamiska och kinetiska data, vilka tidigare har kalibrerats mot experimentella data för bentonit/grundvatten interaktioner.

Resultaten från beräkningarna indikerar att den huvudsakliga alkalinitetsbufferten kommer från föroreningar av karbonatmineral (kalcit) i bufferten, medan jonbytesreaktionerna spelar en underordnad (men inte försumbar) roll. Mängden Ca(II) i det inträngande grundvattnet har betydelse för det slutliga pH-värdet. I Ca(II)rika vatten, typ Äspö, ligger pH i nivå med granitiska grundvatten (7,5-9,5) under hela förvarets funktionstid. I Ca(II)fattiga vatten kommer pH att stiga (10,5-10,8) på grund av förbrukning av kalcit och frigörelse av karbonat.

Systemets reducerande kapacitet styrs huvudsakligen av bentonitens pyritinnehåll, även om innehållet av Fe(II) i montmorilloniten och i karbonater inte kan försummas. Reducerande förhållanden är garanterade i bentonit/grundvatten systemet för hela förvarets livslängd.

Contents

1 Introduction

The KBS-3 design for the final repository of spent nuclear fuel will use MX-80 Wyoming bentonite as buffer material as shown in Figure 1-1. The bentonite buffer material constitutes both a mechanical, hydraulic and chemical barrier in the repository system. The mechanical and hydraulic performance of the bentonite buffer are critically dependent on the integrity of the chemical properties of the clay through the initial thermal and hydraulic gradients imposed in the post-disposal period. Furthermore, any groundwater entering in contact with the canister/spent fuel system will be conditioned by the chemical processes occurring at the bentonite/pore water interface. Consequently, the chemical stability of the near field, this is the alkalinity and redox buffering capacity, will be firstly controlled by the bentonite/groundwater interactions.

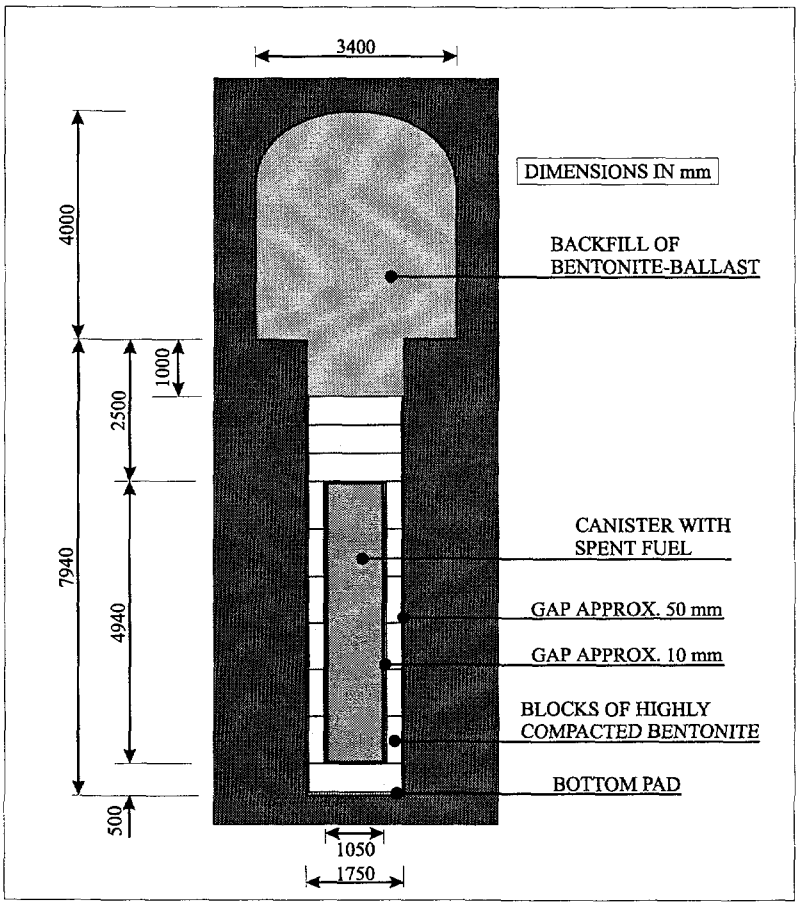

Figure 1-1. *Waste emplacement design and geometry of the KBS-3 type repository.*

The main chemical processes imposed by the bentonite buffer and its very critical accessory minerals and impurities minerals are:

- Alkalinity buffering by the calcite precipitation and dissolution, as well as, Ca-Na ion exchange processes. Na cycling in the system is also linked to the dissolution of the halite which precipitates as a result of the pretreatment of the bentonite.

- Reducing capacity buffering by the pyrite, Fe(II) content in the montmorillonite and siderite contents of the MX-80 bentonite.

- Sulphate cycling due to the dissolution and precipitation of the anhydrite and gypsum content and also linked to the redox cycling through pyrite oxidation.

The main objective of this report is to quantitatively discuss the chemical evolution of the intruding groundwater as a result of the interactions with the MX-80 bentonite main components and accessory minerals. The degradation of the bentonite buffer material is only considered as a result of these chemical inetractions and its is mainly restricted to the dissolution/precipitation of accessory minerals and ion exchange processes in the montmorillonite.

2 Wyoming MX-80 bentonite geochemical properties

The Wyoming MX-80 bentonite considered by SKB as a potential clay buffer is mainly Na-montmorillonite with a content of around 75 wt.%. Other major components are: plagioclase (5 to 8 wt.%), quartz (10 to 15 wt.%), and minor amounts of pyrite, calcite, halite, anhydrite, and other clay minerals, such as kaolinite and illite. Mineralogical, chemical and physical data of the MX-80 bentonite are summarised in Table 2-1.

Table 2-1. Geochemical data for MX-80 bentonite.

Property	Value	Reference
Cation Exchange Capacity (CEC)	85.0 meq/100g	1
Edge sites (OH groups)	2.8 meq/100g	1
Exchangeable Na	81.7 %	2
Exchangeable Mg	3.9 %	2
Exchangeable Ca	14.1 %	2
Exchangeable K	0.3 %	2
Total carbonate ($CaCO_3$)	1.4 wt. %	2
Total quartz (SiO_2)	10 wt. %	3
Total pyrite (FeS_2)	0.3 wt. %	8
$CaSO_4$ impurities	0.34 wt. %	4
NaCl impurities	0.007 wt. %	4
Plagioclase (Mainly albite)	5 to 9 wt. %	1, 5, & 6
Illite	0 to 4 wt. %	1 & 6
Kaolinite	<1 to 7 wt. %	1 & 6

1: Wieland et al. (1994), 2: Müller-Vonmoos and Kahr (1985), 3: van Olphen and Fripiat (1979), 4: Wanner et al. (1992). 5: SKI SITE-94 (1996), 6: Lajudie et al. (1995).

3 The role of bentonite as a chemical buffer

The main chemical function of the bentonite barrier is to provide a large alkalinity and redox buffer capacity.

The alkalinity buffer capacity is mainly given by the following processes:

- Dissolution of the calcite content of the MX-80 bentonite, which is typically around 1.4 wt.%, by the chemical reaction:

$$CaCO_3(s) + H^+ \rightarrow Ca^{2+} + HCO_3^-$$

- Ion exchange reactions between protons and the cations present at the interstitial layers, mainly the replacement of Na^+ present in the bentonite by the Ca^{2+} and Mg^{2+} content of granitic groundwaters. This is represented by the following processes:

$$NaX + K^+ \leftrightarrow KX + Na^+$$
$$2\,NaX + Ca^{2+} \leftrightarrow CaX_2 + 2\,Na^+$$
$$2\,NaX + Mg^{2+} \leftrightarrow MgX_2 + 2\,Na^+$$

- Surface protonation reactions at the edge silanol and aluminol sites, which are exemplified by the equilibria:

$$SOH + H^+ \leftrightarrow SOH_2^+$$
$$SOH \leftrightarrow SO^- + H^+$$

- Montmorillonite weathering reactions.

The first three processes are relatively fast and reversible reactions and can be represented by their thermodynamic properties (Bruno, 1997). The weathering of montmorillonite is a slower and non-reversible, hence it constitutes a kinetic buffering capacity. These processes are very similar to the ones buffering the alkalinity of soils, where distinctions between thermodynamic and kinetic buffer capacities are also made.

The redox buffering capacity of the MX-80 bentonite is mainly provided by its pyrite contain. This redox capacity is given by the reaction:

$$FeS_2(s) + 3.75\,O_2(g) + 1.5\,H_2O \rightarrow Fe(OH)_3(s) + 2\,SO_4^{2-} + 4\,H^+$$

This is a non-reversible process, (in the absence of sulphate reducing bacteria). Hence, it constitutes a kinetic redox buffering capacity.

Although the pyrite content is somewhat variable in the MX-80 bentonite, the average value falls around 0.3 wt.%.

A further redox buffering capacity in the MX-80 bentonite material is provided by the siderite ($FeCO_3$) content as a result of Fe(II) replacement in Mg/Ca carbonates (calcite and dolomite). This is a very labile redox capacity and can be treated thermodynamically. The chemical process is described as:

$$FeCO_3(s) + 0.25\ O_2(aq) + 2.5H_2O \leftrightarrow Fe(OH)_3(s) + H^+ + HCO_3^-$$

Typical Fe(II) substitution in carbonates are in the range between 0.01 to 0.13 expressed as molar fraction of the carbonate content (Deer et al, 1992).

In order to study the long term evolution of the groundwater reacting with the bentonite material and the role of bentonite as a chemical buffer we need to have a consistent thermodynamic and kinetic representation of its chemical behaviour and the bentonite/groundwater interactions.

Most of the models developed to simulate the composition of the groundwater after contacting bentonite can be classified into two different groups:

- Models based on ionic exchange processes (Wieland et al. 1994, Wanner et al. 1992, Olin et al. 1995)

- Models based on the equilibrium of Na-montmorillonite with the groundwater. These models require of the estimation of a solubility constant value for Na-montmorillonite. Due to the variability of compositions of this mineral, solid solution approaches have been usually followed in order to estimate the solubility constant for this solid (Fritz et al., 1985).

Any model to be used to predict the long term evolution of the near field hydrochemistry for performance assessment purposes requires a thorough process of calibration against the available experimental data concerning bentonite/groundwater interactions.

In a first approach we have tried to reproduce experimental data from water-bentonite equilibration experiments in order to constrain the most likely processes controlling this interaction and to obtain the best physico-chemical parameters for the bentonite buffer behaviour. Later we predict the likely chemical evolution of the bentonite/groundwater systems by using these parameters in our geochemical modelling. To do this, we have used the PHREEQC code Parkhurst (1995) in conjunction with the wateq4f.dat database Parkhurst (1995) adding the required solution and mineral data as described in the text.

4 Background of bentonite/groundwater chemical interactions

Werme (private communication 1992) reports a series of experiments performed to quantify bentonite/groundwater (the experimental data are reported in Wanner 1992). In the experiments, a natural Na-bentonite (MX-80) from Wyoming was used. The bentonite was reacted with deionised water and with a synthetic granitic groundwater (Allard water) at high bentonite/water ratio, by applying external pressure. The composition of the final waters equilibrated with bentonite are shown in Table 4-1.

Table 4-1. Experimental data of solution composition after reaction of Na-bentonite with Allard water, from Wanner et al. (1992) after Werme (priv. comm. 1992). Data in mole/dm3, except Alk (eq/dm3). Solid/water ratio was 1.4 g/cm3.

	Na^+	Ca^{2+}	Mg^{2+}	Cl^-	SO_4^{2-}	Alk	pH
Initial Allard water	$2.26 \cdot 10^{-3}$	$4.64 \cdot 10^{-4}$	$1.90 \cdot 10^{-4}$	$1.48 \cdot 10^{-3}$	$1.00 \cdot 10^{-4}$	$1.80 \cdot 10^{-3}$	8.10
Experiment	Na^+	Ca^{2+}	Mg^{2+}	Cl^-	SO_4^{2-}	Alk	pH
60 Allard	$9.13 \cdot 10^{-2}$	$1.00 \cdot 10^{-4}$	$4.12 \cdot 10^{-5}$	$1.92 \cdot 10^{-3}$	$3.54 \cdot 10^{-2}$	$7.33 \cdot 10^{-3}$	9.21
61 Allard	$8.70 \cdot 10^{-2}$	$1.00 \cdot 10^{-4}$	$2.06 \cdot 10^{-5}$	$1.55 \cdot 10^{-3}$	$2.92 \cdot 10^{-2}$	$5.67 \cdot 10^{-3}$	9.29
62 Distilled W	$9.57 \cdot 10^{-2}$	$1.00 \cdot 10^{-4}$	n.d.	$1.72 \cdot 10^{-3}$	$4.06 \cdot 10^{-2}$	$5.00 \cdot 10^{-3}$	9.10
63 Distilled W	$6.96 \cdot 10^{-2}$	$1.00 \cdot 10^{-4}$	n.d.	$1.24 \cdot 10^{-3}$	$2.92 \cdot 10^{-2}$	$3.67 \cdot 10^{-3}$	8.86

n.d.: not determined

The main observed effects of the bentonite equilibration on the water chemistry are:

- Increase in the sodium content, due to the Na-Ca and Na-H exchange in Na-montmorillonite.
- Slight decrease in the calcium content, attributed to a balance between the dissolution of small amounts of gypsum ($CaSO_4$) present in bentonite, calcite dissolution, and the exchange of Na by calcium at the interstitial layers.
- Increase in sulphate content, due to $CaSO_4$ dissolution.
- Increase in alkalinity and pH due to the dissolution of calcite and proton sodium exchange.

These data has been thoroughly interpreted in previous studies by Wanner et al. (1992) and Wieland et al. (1994). These authors proposed a chemical model in order to explain this behaviour. Their model was based on the following assumptions:

- The system was open to air, hence $pCO_2 = 10^{-3.5}$ bar.
- Equilibrium of groundwater with quartz and calcite.
- Magnesium content is attributed entirely to ion exchange reactions within the clay fraction. The presence of dolomite is neglected.
- Sodium chloride and calcium sulphate impurities are assumed to dissolve completely.
- In order to account for the alteration of montmorillonite an ion exchange model involving Na, Ca, K, and Mg is assumed at the interstitial layer sites.
- The effect of the protonation/de-protonation equilibria at the montmorillonite edge sites is considered.
- No redox reactions are included, therefore neither the dissolution of pyrite nor the reduction of $O_2(g)$ are considered

The modelled data of Wanner et al. (1992) and Wieland et al. (1994), based on the above assumptions, are summarised in Table 4-2.

Table 4-2. Modelled data of solution composition after reaction of Na-bentonite with Allard water, from Wanner et al. (1992) and Wieland et al. (1994). Data in mole/dm3, except Alk (eq/dm3). Solid/water ratio was 1.4 g/cm3.

Source	Na^+	Ca^{2+}	Mg^{2+}	Cl^-	SO_4^{2-}	Alk	pH
Experiments in Allard groundwater							
Wanner et al. (1992)	$7.5 \cdot 10^{-2}$	$7.8 \cdot 10^{-5}$	$2.0 \cdot 10^{-5}$	n.d.	n.d.	$8.0 \cdot 10^{-3}$	9.0
Wieland et al. (1994)	$7.7 \cdot 10^{-2}$	$1.4 \cdot 10^{-3}$	$3.9 \cdot 10^{-4}$	$1.7 \cdot 10^{-3}$	$3.0 \cdot 10^{-2}$	$3.4 \cdot 10^{-3}$	8.4
Experiments in bidistilled water							
Wanner et al. (1992)	$8.2 \cdot 10^{-2}$	$1.0 \cdot 10^{-4}$	n.r.	n.r.	n.r.	$7.1 \cdot 10^{-3}$	8.9
Wieland et al. (1994)	$7.6 \cdot 10^{-2}$	$1.4 \cdot 10^{-3}$	$3.9 \cdot 10^{-4}$	$1.6 \cdot 10^{-3}$	$3.0 \cdot 10^{-2}$	$3.4 \cdot 10^{-3}$	8.4

n.r.: not reported.

By looking into the previous graphs and Tables, we can see that the best agreement with the experimental observations is obtained in the case of experiments performed with Allard groundwater by using the model proposed by Wanner et al., 1992. However, this model predicts a pH value which is 0.3 units below the measured one. In the case of the experiments performed with distilled water, a similar agreement is obtained by the two models.

By using the models described, the same authors (Wanner et al., 1992 and Wieland et al., 1994) calculated the evolution of a closed system through the bentonite buffer. The authors estimated a period of 13,800 years for the total porewater replacement, based on the hydraulic conductivity of clay (10^{-11} m/s), the thickness of the bentonite wall (0.35 m), and a hydraulic gradient of 0.1.

In both cases the main features outlined are the substitution of Na by Ca in the montmorillonite and a very fast calcite consumption, which is a continuous source of Ca for the bentonite substitution. The relative rates at which both processes take place depend on the water composition and the bentonite exchange model considered. For a more diluted groundwater, calcite saturation is obtained at shorter contact times and therefore Na-Ca exchange in the bentonite is restricted by the availability of Ca from the contacting groundwater.

The comparison with the experimental data is shown in the Figures 4-1 and 4-2.

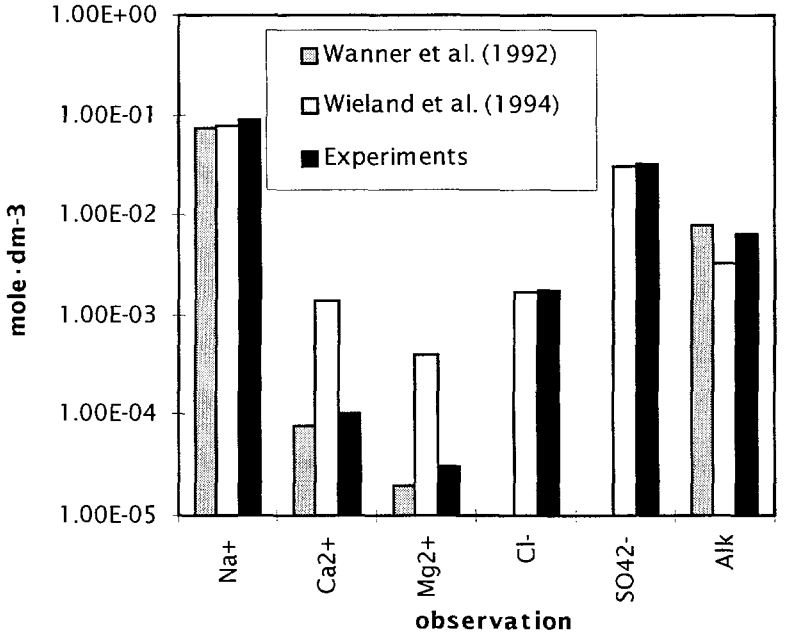

***Figure 4-1**. Experiments conducted with Allard groundwater.*

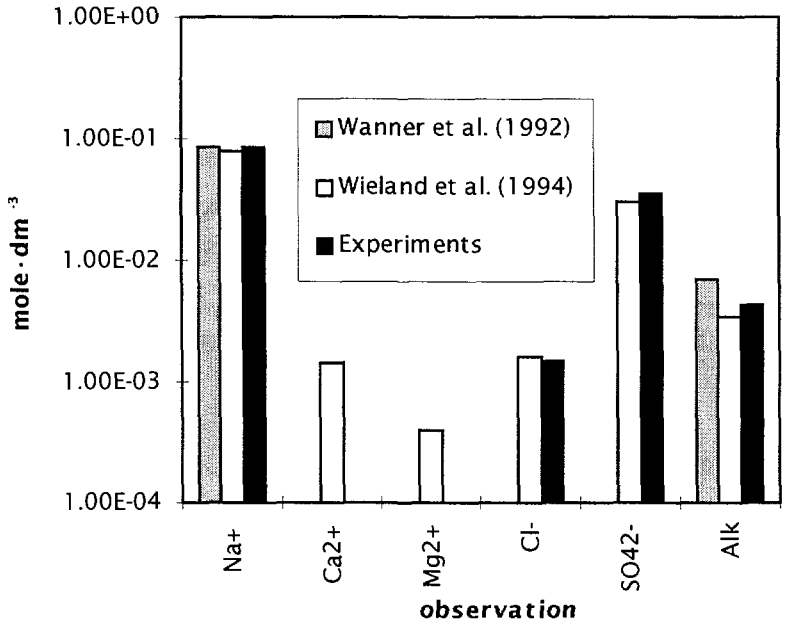

Figure 4-2. *Experiments conducted with distilled groundwater.*

5 Calibration of the model with experimental data

In order to perform the model calibration, we have considered two different sets equilibrium constants to describe the ion exchange reactions. The first data set is the one proposed by Wieland et al. (1994) while the second one is a slightly different data set from Olin et al. (1995). The surface acidity constants are taken from the surface titrations of montmorillonite run by Wieland et al. (1994), as the only experimental source available.

The mineralogical and chemical parameters considered in our calculations are as follows:

- The groundwater is equilibrated with Calcite and Quartz, the maximum calcite and quartz contents assumed in the bentonite are:

  Maximum Calcite: 1.4wt. %
  Maximum Quartz: 10 wt. %

- The system is assumed to be in equilibrium with the atmospheric $CO_2(g)$, hence:

  $$pCO_2(g) = 10^{-3.5} \text{ atm}$$

- We assumed that the initial gypsum and halite content is totally dissolved. The maximum contents of these accessory minerals are:

  Maximum NaCl: 0.007wt. %
  Maximum $CaSO_4$: 0.34wt. %

- The following ion-exchange equilibria and equilibrium constants are used. The value of the constants slightly changes depending on the authors.

  $2\,XNa + Ca^{2+} \Leftrightarrow X_2Ca + 2\,Na^+$; $\log K_{Na/Ca} = 2.10^a, 1.6^b$

  $2XNa + Mg^{2+} \Leftrightarrow X_2Mg + 2\,Na^+$; $\log K_{Na/Mg} = 1.50^a, 1.3^b$

- The surface acidity equilibria (no electric double layer considered) and equilibrium constants are:

  $SOH + H^+ \Leftrightarrow SOH^{2+}$; $\log K_+ = 5.40^b$

  $SOH \Leftrightarrow SO^- + H^+$; $\log K_- = -6.70^b$

  [a]. Olin et al., 1995; [b]. Wanner et al.,1992.

Only in the case of Wanner et al, 1992, the surface acidity equilibria are considered.

The results of the calculations are shown in Table 5-1.

Table 5-1. Modelled data of solution composition after reaction of Na-bentonite with Allard water and distilled water. Data in mole/dm3, except Alk (eq/dm3). Solid/water ratio was considered as 1.4 g/cm3.

Exchange Source	Na^+	Ca^{2+}	Mg^{2+}	Cl^-	SO_4^{2-}	Alk	pH
Experiments in Allard groundwater							
Olin et al. (1994)	$1.19 \cdot 10^{-1}$	$1.14 \cdot 10^{-4}$	$9.03 \cdot 10^{-5}$	$3.15 \cdot 10^{-3}$	$3.51 \cdot 10^{-2}$	$5.85 \cdot 10^{-3}$	8.9
Wieland et al. (1994)	$9.92 \cdot 10^{-2}$	$5.03 \cdot 10^{-3}$	$1.28 \cdot 10^{-3}$	$3.15 \cdot 10^{-3}$	$3.51 \cdot 10^{-2}$	$7.76 \cdot 10^{-4}$	8.1
Experiments in distilled water							
Olin et al. (1994)	$1.16 \cdot 10^{-1}$	$1.12 \cdot 10^{-4}$	$8.7 \cdot 10^{-5}$	$1.67 \cdot 10^{-3}$	$3.5 \cdot 10^{-2}$	$6.63 \cdot 10^{-3}$	8.9

These results are plotted in Figures 5-1 and 5-2 in comparison with the experimental data and with the results obtained by Wieland et al. (1994) and Wanner et al. (1992).

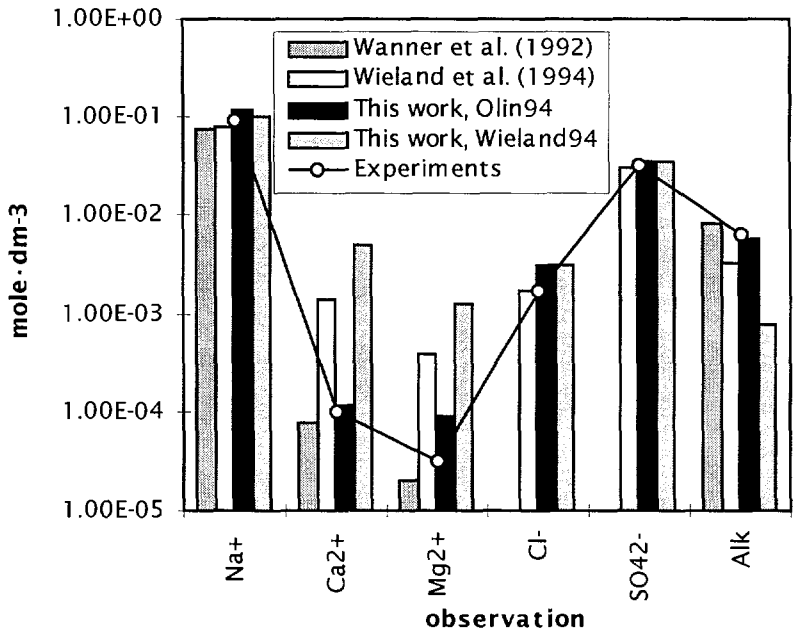

Figure 5-1. *Experiments conducted with Allard groundwater.*

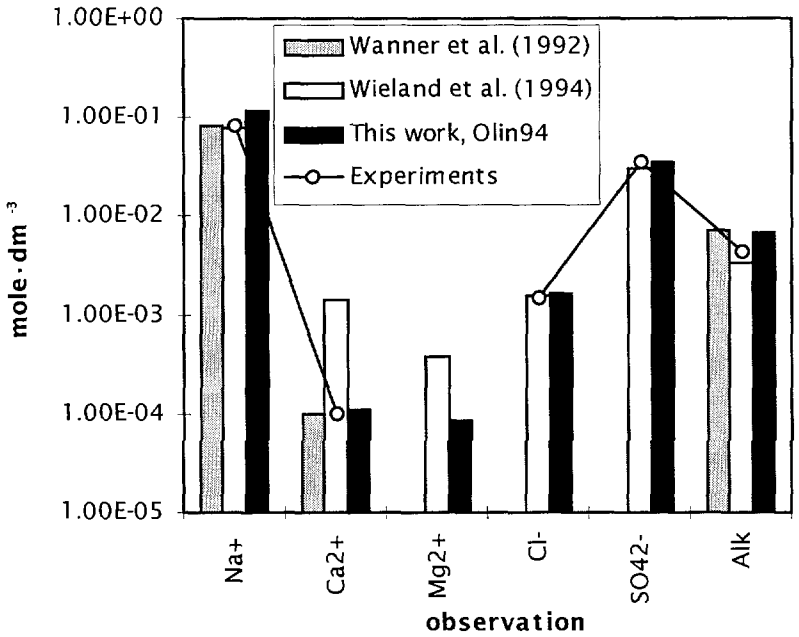

Figure 5-2. *Experiments conducted with distilled water.*

As we can infer from the previous figures, the model calculations using the Olin et al. (1994) exchange constants reproduces a porewater composition which is closer to the experimental measurements as reported by Werme (private communication 1992). We can also notice that the calculated final pH does not differ from the experimentally determined one (see Table 4-1). Some differences are worth to be noticed: the calculated chloride and sodium concentrations are slightly larger than the experimental values. This can be attributed to differences in the original amount of halite in the bentonite.

It can be also observed that we have not considered equilibrium with any aluminium bearing phases. This is mainly due to the fact that no data on aluminium concentrations of the groundwater after the equilibration with bentonite has been reported in the experiments.

6 Selection of the interacting groundwater

Once we have established a satisfactory chemical model which is able to explain, within the experimental error, the observed interactions between bentonite and synthetic granitic groundwater, we have to discuss the composition of the various granitic waters which may interact with bentonite. The composition of the reacting groundwater is a key factor in order to ascertain the long term chemical behaviour of the bentonite buffer. Three different granitic groundwaters are being considered in the SR 97' assessment, which reflect the observed compositions at Gideå, Finnsjön and Äspö. The selected water compositions are shown in Table 6-1.

Table 6-1. Selected groundwater compositions. Data in mole/dm^3 as reported in Laaxoharju (1997).

Component	Gideå	Finnsjön	Äspö
Na	$4.57 \cdot 10^{-3}$	$1.20 \cdot 10^{-2}$	$9.13 \cdot 10^{-2}$
K	$5.13 \cdot 10^{-5}$	$5.13 \cdot 10^{-5}$	$2.05 \cdot 10^{-4}$
Ca	$5.25 \cdot 10^{-4}$	$3.55 \cdot 10^{-3}$	$4.73 \cdot 10^{-2}$
Mg	$4.11 \cdot 10^{-5}$	$6.99 \cdot 10^{-4}$	$1.73 \cdot 10^{-3}$
Fe	$8.95 \cdot 10^{-7}$	$3.22 \cdot 10^{-5}$	$4.30 \cdot 10^{-6}$
Mn	$1.82 \cdot 10^{-7}$	$2.37 \cdot 10^{-6}$	$5.28 \cdot 10^{-6}$
H_4SiO_4	$1.67 \cdot 10^{-4}$	$1.99 \cdot 10^{-4}$	$1.46 \cdot 10^{-4}$
HCO_3^-	$2.95 \cdot 10^{-4}$	$4.56 \cdot 10^{-3}$	$1.64 \cdot 10^{-4}$
F^-	$1.68 \cdot 10^{-4}$	$7.89 \cdot 10^{-5}$	$7.89 \cdot 10^{-5}$
Cl^-	$5.01 \cdot 10^{-3}$	$1.56 \cdot 10^{-2}$	$1.81 \cdot 10^{-1}$
SO_4^{2-}	$1.04 \cdot 10^{-6}$	$5.10 \cdot 10^{-4}$	$5.83 \cdot 10^{-3}$
pH	9.3	7.9	7.7
Eh(mV)*	-202 ± 50	-250 ± 50	-308 ± 50

*The standard deviation in the selected Eh values is a result of the uncertainty in the redox `potential determinations (Grenthe et al, 1992).

7 Extrapolation to repository conditions

The expected solid/water ratio is one of the critical factors to consider when applying the bentonite model to repository conditions. In the experiments previously used to calibrate the model, the bentonite/water ratio was 1.4 grams of solid per cm^3 of water. According to Bäckblom (1996), the expected porewater/bentonite ratio in the repository will be 0.41 dm^3 water per dm^3 of bentonite (Table 7-1). The initial accessory mineral composition of the bentonite is shown in Table 7-2.

Table 7-1. Bentonite physical properties.

Property	Value	Reference
Density (highly compacted)	1.59 g/cm^3	Bäckblom (1996)
Density (highly compacted, water saturated)	2.00 g/cm^3	Bäckblom (1996)
Porewater/bentonite ratio	0.41 cm^3/cm^3	Bäckblom (1996)
Bentonite buffer width	35 cm	Bäckblom (1996)

Table 7-2. Starting bentonite composition at repository conditions.

Component	Amount in bentonite (moles/l)
Quartz	8.90
Calcite	0.75
Pyrite	0.13
NaCl	0.0064
Anhydrite	0.13
CaX_2	0.32
NaX	3.69
MgX_2	0.088
KX	0.013

8 Methodology of the calculations

In order to study the long term chemical evolution of the bentonite/groundwater system we have performed 1-D reactive transport calculations. The calculations have been performed by using the PHREEQC code, an extended version of PHREEQE including surface complexation reactions, ionic exchange and advective transport simulations (no diffusion can be considered in this code). In order to simulate the diffusive motion of groundwater in bentonite we calculated the differnces in hydraulic potential at the inlet and outlet of the buffer material, by taking ino consideration the permeability of the buffer material. In this way we could impose to the system and advective flow velocity equivalent to the diffusive flow velocity actually working in the system. A similar aproach has been used by Wanner et al 1992 and Wieland et al 1994. All the calculations are based in 1 kg of water.

We have performed two different types of calculations under repository conditions:

- Bentonite-groundwater equilibration: In this simulation, groundwater is fully and instantaneously equilibrated with bentonite. The final groundwater composition is reported. This is to identify the key chemical processes and to discuss the differences due to the three different groundwater compositions.

- Study of the chemical gradient through the bentonite buffer: After equilibration, water in contact with bentonite is totally replaced by fresh groundwater In this case, the thickness of the bentonite buffer is divided into 5 cells. In this case we attempt to simulate the chemical gradient through the thickness of the buffer.

9 Results

The results obtained in the simulations are presented and discussed in the following sections.

9.1 Bentonite-groundwater equilibration

The following features have been included in order to represent more accurately the repository conditions:

- Presence of pyrite and some sensitivity calculations to explore the role of Fe(II) carbonate impurities in the redox buffering of the system.
- Closed system, no constant CO_2 pressure considered.
- Initial O_2 fugacity given by the background redox condition of the intruding groundwater (Laaxoharju, 1997)

The results of the instantaneous equilibrium calculations are given in Table 9-1.

Table 9-1. Modelled data of solution composition after reaction of Na-bentonite with different groundwaters at repository conditions. Data in mole/dm3. Solid/water ratio was considered as 4.85 g/cm^3. CaX_2, MgX_2, NaX, and KX are the cation concentrations in exchangeable sites.

Component	Äspö		Finnsjön		Gideå	
(moles/l)	Initial	Final	Initial	Final	Initial	Final
Na	$9.13\cdot10^{-2}$	$5.59\cdot10^{-1}$	$1.20\cdot10^{-2}$	$4.22\cdot10^{-1}$	$4.57\cdot10^{-3}$	$4.13\cdot10^{-1}$
K	$2.05\cdot10^{-4}$	$4.96\cdot10^{-4}$	$5.13\cdot10^{-5}$	$3.59\cdot10^{-4}$	$5.13\cdot10^{-5}$	$3.51\cdot10^{-4}$
Ca	$4.73\cdot10^{-2}$	$3.71\cdot10^{-3}$	$3.55\cdot10^{-3}$	$2.04\cdot10^{-3}$	$5.25\cdot10^{-4}$	$1.96\cdot10^{-3}$
Mg	$1.73\cdot10^{-2}$	$2.34\cdot10^{-3}$	$6.99\cdot10^{-4}$	$1.39\cdot10^{-3}$	$4.11\cdot10^{-5}$	$1.33\cdot10^{-3}$
Fe	$4.30\cdot10^{-6}$	$4.56\cdot10^{-6}$	$3.22\cdot10^{-5}$	$3.22\cdot10^{-5}$	$8.95\cdot10^{-7}$	$1.13\cdot10^{-6}$
H_4SiO_4	$1.46\cdot10^{-4}$	$8.90\cdot10^{-5}$	$1.99\cdot10^{-4}$	$9.28\cdot10^{-5}$	$1.67\cdot10^{-4}$	$9.30\cdot10^{-5}$
HCO_3^-	$1.64\cdot10^{-4}$	$4.70\cdot10^{-2}$	$4.56\cdot10^{-3}$	$6.38\cdot10^{-2}$	$2.95\cdot10^{-4}$	$6.30\cdot10^{-2}$
Cl	$1.81\cdot10^{-1}$	$1.87\cdot10^{-1}$	$1.56\cdot10^{-2}$	$2.20\cdot10^{-2}$	$5.01\cdot10^{-3}$	$1.14\cdot10^{-2}$
SO_4^{2-}	$5.83\cdot10^{-3}$	$1.36\cdot10^{-1}$	$5.10\cdot10^{-4}$	$1.30\cdot10^{-1}$	$1.04\cdot10^{-6}$	$1.30\cdot10^{-1}$
pH	7.7	6.7	7.9	6.8	9.3	6.9
Eh (mV)	-118	-132	-118	-137	-118	-145

The main features can be observed in Table 9-2.

Table 9-2. Main differences observed after instantaneous equilibrium calculations

Component (moles/l)	Initial	Äspö		Finnsjön		Gideå	
		Final	Variation	Final	Variation	Final	Variation
Calcite	0.75	0.69	$-5.8\cdot10^{-2}$	0.68	$-7.1\cdot10^{-2}$	0.68	$-7.4\cdot10^{-2}$
Pyrite	0.13	0.13	$-2.6\cdot10^{-7}$	0.13	$-5.3\cdot10^{-8}$	0.13	$-2.4\cdot10^{-7}$
Quartz	8.90	8.90	$+5.7\cdot10^{-5}$	8.90	$+1.1\cdot10^{-4}$	8.90	$+7.4\cdot10^{-5}$
Anhydrite	0.13	0.0	-0.13	0.0	-0.13	0.0	-0.13
Halite	$6.4\cdot10^{-3}$	0.0	$-6.4\cdot10^{-3}$	0.0	$-6.4\cdot10^{-3}$	0.0	$-6.4\cdot10^{-3}$
NaX	3.69	3.23	-0.46	3.29	-0.40	3.29	-0.40
CaX_2	0.32	0.55	+0.23	0.52	+0.20	0.52	+0.20
MgX_2	$8.8\cdot10^{-2}$	$8.7:10^{-2}$	$-6.3\cdot10^{-4}$	$8.7:10^{-2}$	$-7.1\cdot10^{-4}$	$8.7:10^{-2}$	$-1.3\cdot10^{-3}$
KX	$1.3\cdot10^{-2}$	$1.3\cdot10^{-2}$	$-2.9\cdot10^{-4}$	$1.3\cdot10^{-2}$	$-3.1\cdot10^{-4}$	$1.3\cdot10^{-2}$	$-3.0\cdot10^{-4}$

A comparison of the effect on groundwater composition as a result of the interaction with MX-80 Wyoming bentonite is given in Figures 9-1 through 9-6.

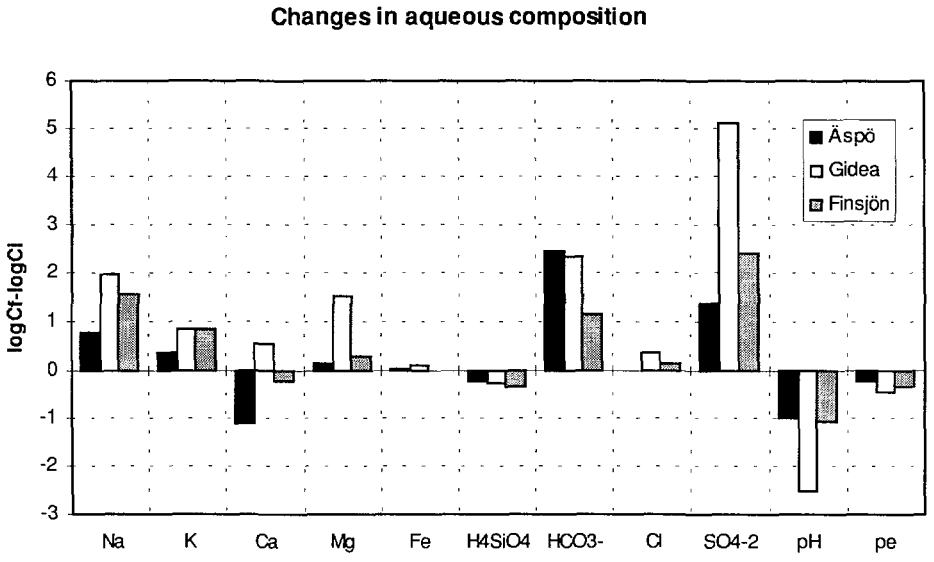

Figure 9-1. *Changes in aqueous composition (given as the difference between logarithms) for the three reference groundwaters as a result of the interaction with MX-80 bentonite.*

By looking at Figure 5, we may observe that there is a general increase on cationic concentrations, except for the Ca(II) content from Äspö groundwater, the bicarbonate concentration increases almost two logarithmic units for Äspö and Gideå groundwater. In the case of Finnsjön it only increases one order of magnitude. Sulphate concentration is largely increased when Gideå groundwater dissolves the anhydrite content of bentonite. Äspö groundwater is affected to a lesser extent due to its initially large content. The interaction of the MX-80 bentonite with the three groundwater types decreases the pH and pe of the reacting waters, mainly as a consequence of the oxidation of pyrite. This decrease in pH has been observed by some authors (Sasaki et al., 1995) when equilibrating groundwater with pyrite-bearing bentonite. Again, Gideå groundwater shows a larger effect because of the combination of high pH and relatively low bicarbonate concentration resulting in a lower pH buffer capacity.

Concerning, the effect of the different intruding groundwaters on the chemical composition of the bentonite, we can draw some general statements by looking into Table 9-1:

- The general effect of the groundwater equilibration on the ionic exchange characteristics of the bentonite is a net exchange of Na(I) and to a lesser extent the Mg(II) by Ca(II).

- The effect on the accessory minerals or bentonite impurities is a 1% depletion of the calcite content an insignificant depletion of the pyrite content and the complete wash out of the soluble anhydrite and halite content. The calculations also indicate a tendency towards a slight precipitation of quartz. The different compositions of the three reacting groundwaters do not have a marked effect on the bentonite composition.

9.2 Time evolution of the bentonite-groundwater system

In this case, after equilibrium of water with bentonite is achieved according to the previous calculations, the porewater is totally replaced with new incoming groundwater. The evolution of the chemistry of the water and the minerals remaining in the buffer are recorded continuously during a number of exchange cycles.

The hydraulic conductivity of compacted bentonite depends on its density at water saturation, but ranges from $2 \cdot 10^{-14}$ m/s at 2.1 g/cm^3 density to 10^{-10} m/s at 1.2 g/cm^3 of density. Due to these low values of hydraulic conductivity, the migration of the water constituents through the bentonite medium is mainly controlled by diffusion. From different diffusion estimates, a hypothetical water flow leaving the near field, $Q_{eq} = 2 \cdot 10^{-4}$ m^3/year has been proposed (SITE 94). This implies total replacement of the bentonite porewater after 10,000 years.

We have performed calculations by replacing the initial porewater of the system 300 times. This is equivalent to study the evolution of the system during a minimum of 3,000,000 years.

We have performed an analysis of what would be the effect of an intrusion of oxidants in the system. Three different redox conditions in the intruding groundwater have been considered:

- The base case scenario where the redox condition is the result of the bentonite/groundwater interactions. This is denoted as pe calculated.

- In this case we study the evolution at the postclosure when remanent oxygen fugacities can be at the atmospheric level log $fO_2(g) = -0.7$ This calculation is performed in order to determine the time it takes to the near field hydrochemistry to return to unperturbed levels.

- This case is quite unreasonable and it is the result of some scoping calculations that indicated excess oxygen constant resulting from O_2 bubbles trapped in ice during a glaciation period (SITE 94). This is denoted in the graphsas log $fO_2(g) = -0.22$ According to recent work, this extreme oxygen fugacities, are very unlikely to reach repository level due to the reducing capacity of the bedrock and conductive fractures (Guimerà et al, 1998). However, we have kept these values as a test for the extent on the redox buffer capacity of the bentonite/groundwater system to react in very extreme conditions.

In the previous chemical analysis we have identified calcite and pyrite as the key accessory minerals which control the alkalinity and redox capacity of the bentonite/pore water system.. Therefore in these calculations we have performed an additional sensitivity analysis by varying the content of these impurities within the ranges established for MX-80 bentonites. This variation has been coupled to the chemistry of the various groundwater compositions as follows:

- In the calculations with Äspö groundwater: we have assumed 0.3 wt.% of calcite and 0.01 wt.% of pyrite.

- In the calculations with Finnsjön groundwater: we have assumed 0.75 wt.% of calcite and 0.01 wt.% of pyrite.

- In the calculations involving Gideå groundwater: we have assumed 1.5 wt.% of calcite and 0.01 wt.% of pyrite.

The average contents in MX-80 bentonite according to the mineralogical characterisation are 0.3 wt.% of calcite and 0.01 wt.% of pyrite. However, in the calculations for Finnsjon and Gideå, the calcite contents were increase in order to perform a sensitivity study on the calcite depletion and the corresponding impact on the near field aqueous chemistry.

In the cases were we have used the maximum partial O_2 pressure (log pO_2 = -0.22) one additional calculation has been done by increasing calcite and pyrite contents up to 1.4 wt. % and 0.3 wt. %.

The evolution of the systems is presented in Figures 9-2 to 9-4.

9.2.1 Evolution of the master variables pH and pe

9.2.1.1 Results from Äspö groundwater: (Figure 9-2)

As we have previously discussed, the proton balance at the bentonite pore water is mainly controlled by calcite, pyrite and the surface of montmorillonite. While, pyrite oxidation is responsible of the initial acidification of the system, the calcite content is essential to buffer this effect. This is visible in Figure 9-2, where the time dependent diagrams for the evolution of the pH and pe are shown up to 1,000,000 years. The initial pH and Eh variation after 125,000 years are the result of the total replacement by the granitic groundwater of the distilled water previously introduced in the bentonite during the pre-saturation phase. This is clearly an artefact from the way the calculations are made and does not represent the evolution of the buffer material under operational conditions. Further changes in the pe of the system are the result of the exhaustion of the pyrite content in the bentonite when oxic waters are introduced in the system. When unreasonably high oxygen fugacities (log fO_2 = -0.22) are assumed the average pyrite content is depleted after some 300,000 years. However, if the pyrite content is assumed to be in the higher range of what it has been measured (% weight= 0.3) the reducing capacity of the buffer system is maintaned even in this very unlikely circumstances. Atmospheric fugacities (log fO_2 = -0.70) would only have an impact if the post closure period is extended for some 750,000 years, which is a rather unlikely possibility.

In the base case, the resulting values of pH and Eh are only affected by the replacement by the granitic groundwater of the distilled water after some 125,000 years, resulting in an initial increase in alkalinity, which gradually evolves into pH values which correspond to the ones given by the intruding granitic groundwater. The reducing capacity of the system is basically not affected by the reaction with granitic groundwater as the reox gradients are small (both the bentonite pore water and the groundwater have low Eh).

Specifically, in the case of simulating the interaction of bentonite with Äspö groundwater. The input of Ca(II) due to the large concentrations in Äspö groundwater induces not only the exchange of Na by Ca in the bentonite, but also the precipitation of calcite. This calcite acts buffering the alkalinity of the system and keeps the pH levels above 8, ensuring the chemical integrity of the bentonite buffer material.

In terms of the redox evolution, the simulations indicate that the reducing capacity of the bentonite system would only be exhausted after 300,000

years, if a continuous flow of Äspö groundwater equilibrated with the atmosphere would be reacting with bentonite with the lowest pyrite content.

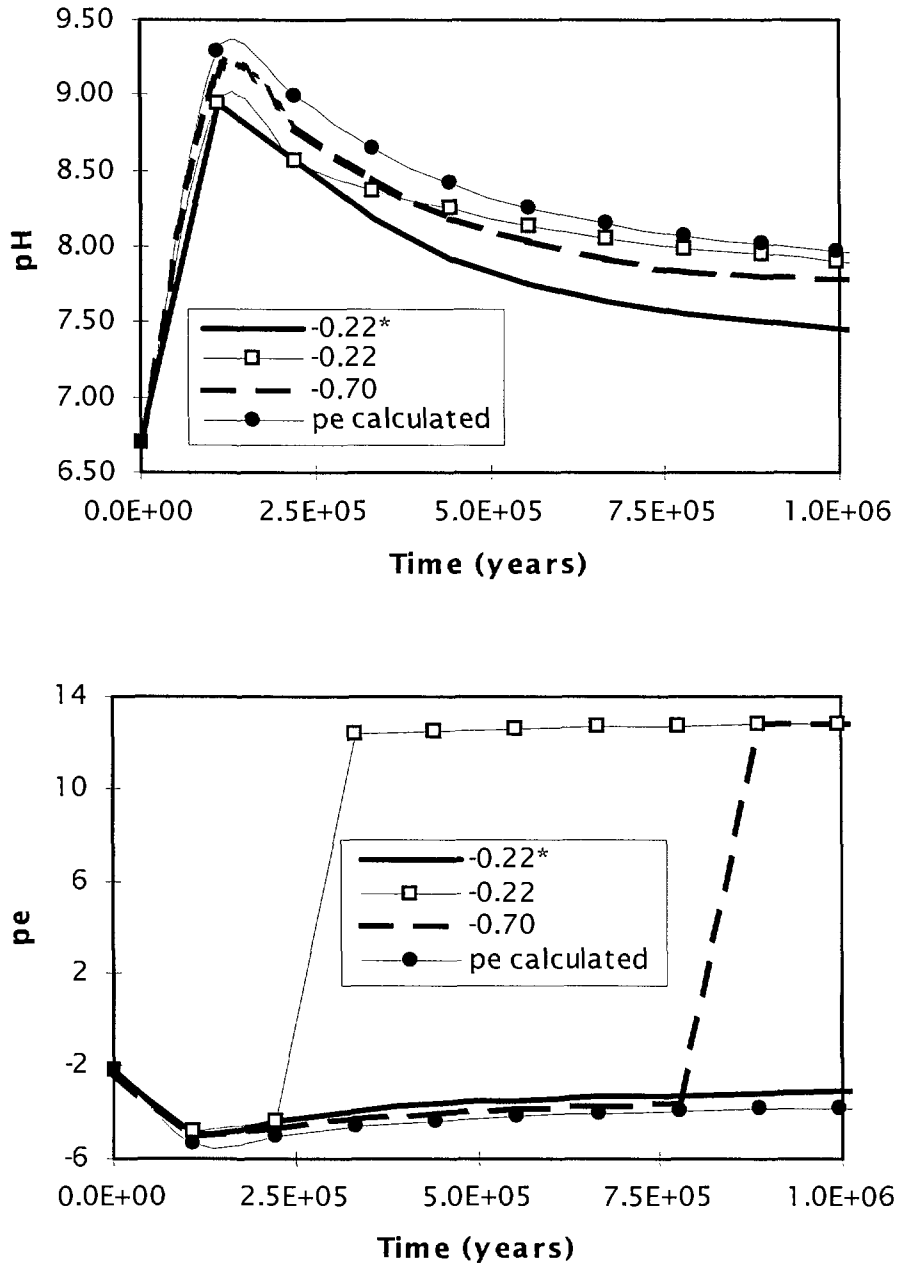

Figure 9-2. *Time-dependent diagrams for the evolution of the Äspö groundwater/bentonite interaction. Curves correspond to different partial oxygen pressures. Initial calcite and pyrite amounts: 0.3 wt % and 0.01 wt % respectively, except for the curve of log fO_2= -0.22* where calcite and pyrite amounts are 1.4 wt. % and 0.3 wt. % respectively. pe calculated stands for the cases where the oxygen fugacity is obtained from the groundwater redox potential. (for the sake of clarity only results up to 1 million years are shown.)*

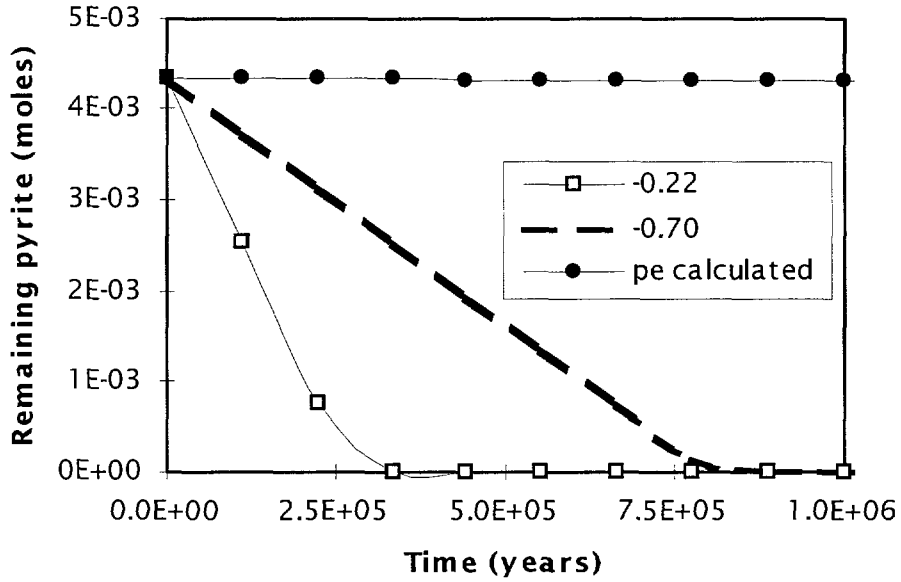

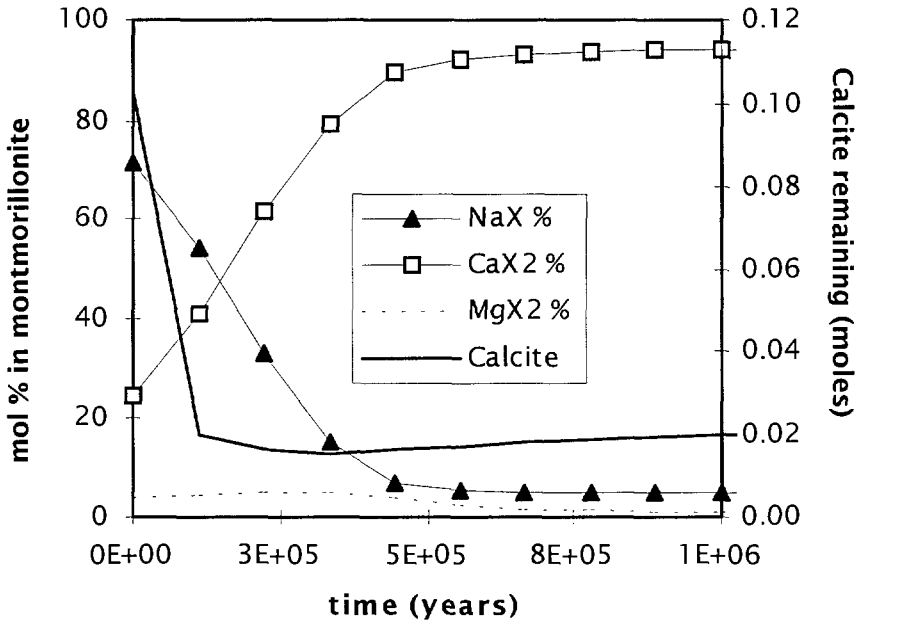

Figure 9-2. (cont.)

It is also interesting to notice that the substitution of Na by Ca in montmorillonite occurs at around 500.000 years in all cases, since it only depends on the calcite content and the calcium concentration in groundwater.

9.2.1.2 Results from Finnsjön groundwater: (Figure 9-3)

The initial calcium content in Finnsjön is lower than in Äspö groundwater, however, the large bicarbonate content of this water causes the initial

precipitation of calcite. Further water contact induces the exchange of Na by Ca and the system becomes undersaturated with respect to calcite. This causes the total exhaustion of the calcite content. This phenomenon is illustrated by the different final exchange sites composition in bentonite: whereas in Äspö nearly all sodium bentonite has been converted into calcium bentonite after 0.5 million years, while this effect is not observed in Finnsjön after 2 million years. The net effect of this in the pH evolution of the system is a relatively sharp recovery of high alkalinity levels at the initial contact times with a resulting pH ranging between 9-10. This situation is kept for the first 1 million years of contact.

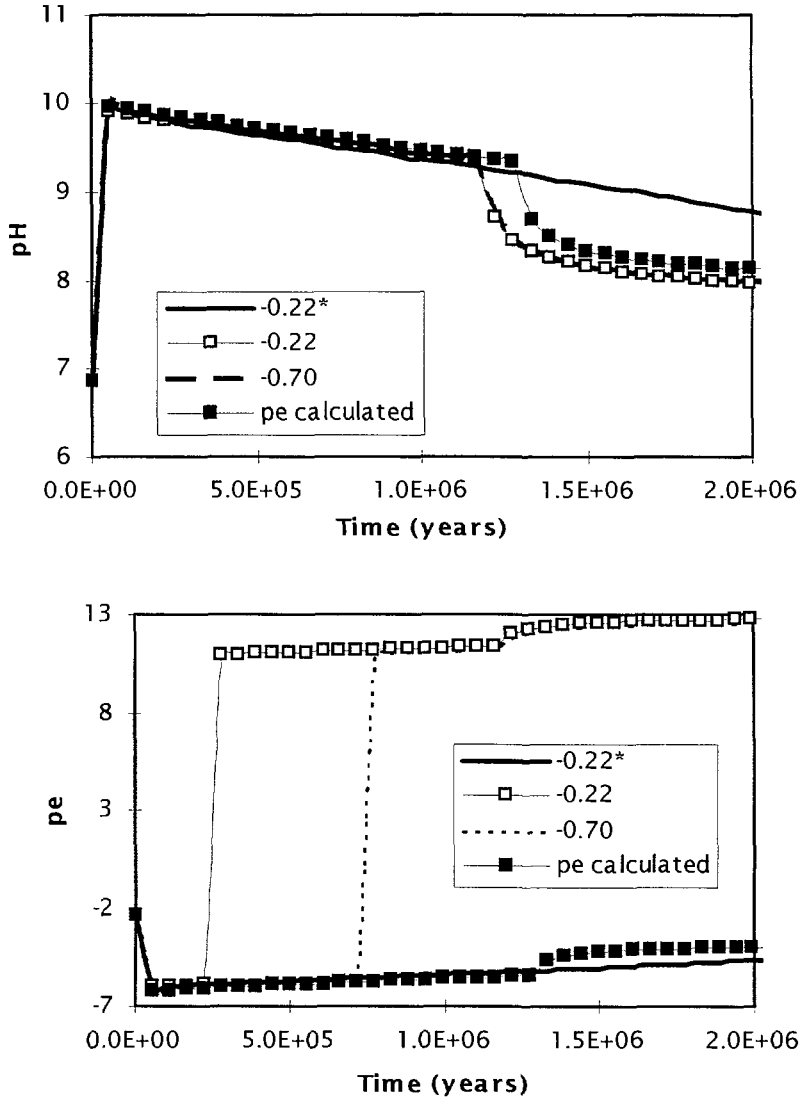

Figure 9-3. *Time-dependent diagrams for the evolution of the Finnsjön groundwater/bentonite interaction. Initial calcite and pyrite content: 0.75 wt% and 0.01 wt% respectively, except for the case with log pO_2= -0.22* where calcite and pyrite fractions are considered to be 1.4 wt% and 0.3 wt% respectively. In order to observe the some changes in the system, results are shown up to 2 million years in this case.*

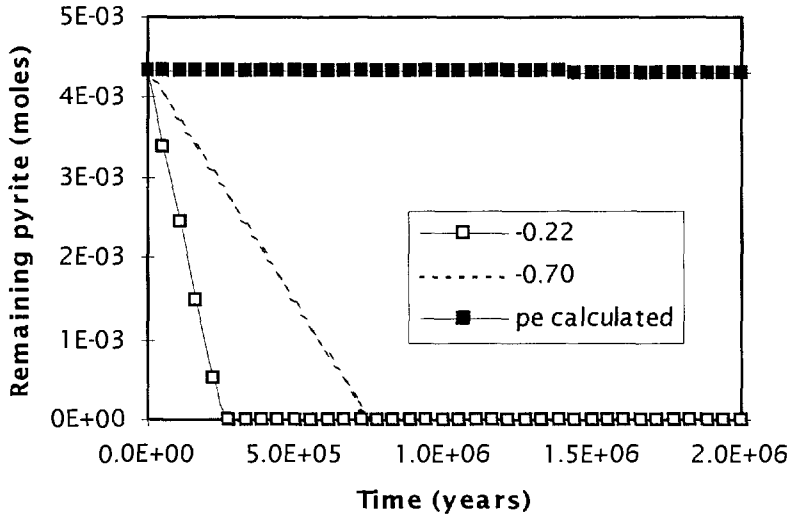

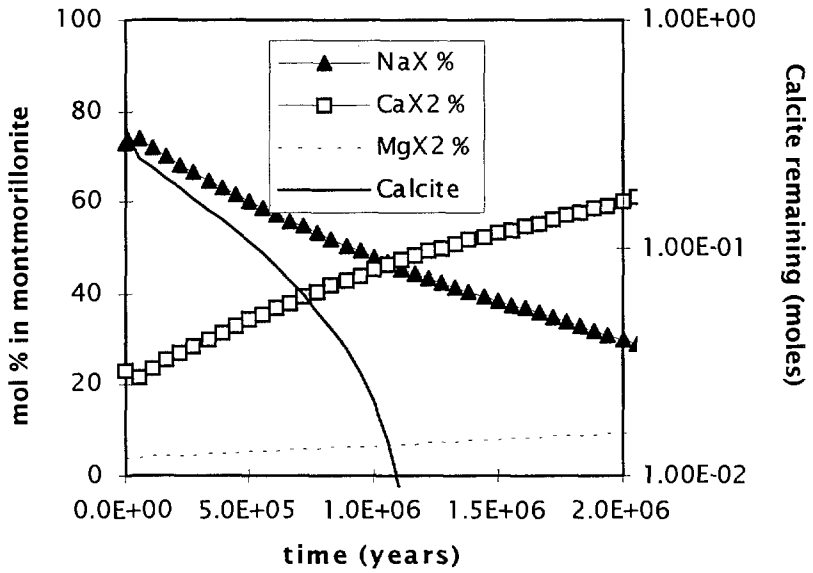

Figure 9-3. (cont.)

The evolution of the redox conditions is very similar to the one observed with Äspö groundwaters. However, pyrite is exhausted at relatively shorter times (400 hundred thousand vs. 500 thousand years) in the case of Finnsjön. This is due to the fact that the pH is higher in the case of interacting with Finnsjön groundwaters due to their larger bicarbonate content. However, the essential fact is that the reducing capacity of the system is ensured for the bentonite system up to some 200,000 years, even in the case when equilibrium with the atmosphere is assumed.

9.2.1.3 Results from Gideå groundwater: (Figure 9-4)

The evolution pattern of the bentonite pore water system interacting with Gideå groundwater presents is similar to the one observed by considering Finnsjön groundwater. However, there is an important difference in the

evolution of the alkalinity of the system and the associated pH values. Because Gideå groundwater has a relatively low Ca(II) content there is a fast depletion of the calcite content which cannot be compensated by the slower Na-Ca exchange. This results in an increase in the resulting pH to values over 10.5. Although, we do not have any experimental observation confirming this behaviour in low calcium content waters, we have no reason to doubt of these results as the chemical model used has been properly calibrated in the previous sections

The reducing capacity of the bentonite system behaves in the case of Gideå groundwater similarly to Finnsjön and reducing conditions are ensured for at least some hundred thousand years in atmospheric conditions even assuming the lowest pyrite content.

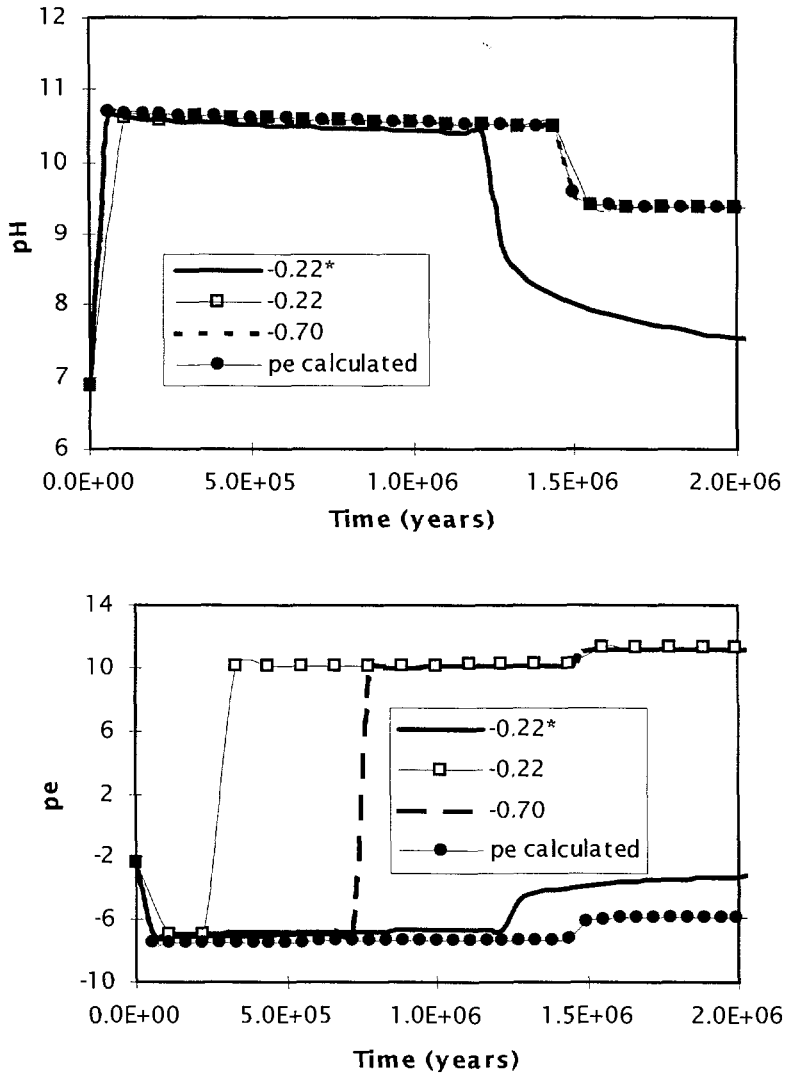

Figure 9-4. *Time-dependent diagrams for the evolution of the Gideå groundwater/bentonite interaction. Initial calcite and pyrite amounts of 1.5 wt. % and 0.01 wt. % respectively, except for the curve of log pO_2= -0.22* where calcite and pyrite amounts are 1.4 wt. % and 0.3 wt. % respectively.*

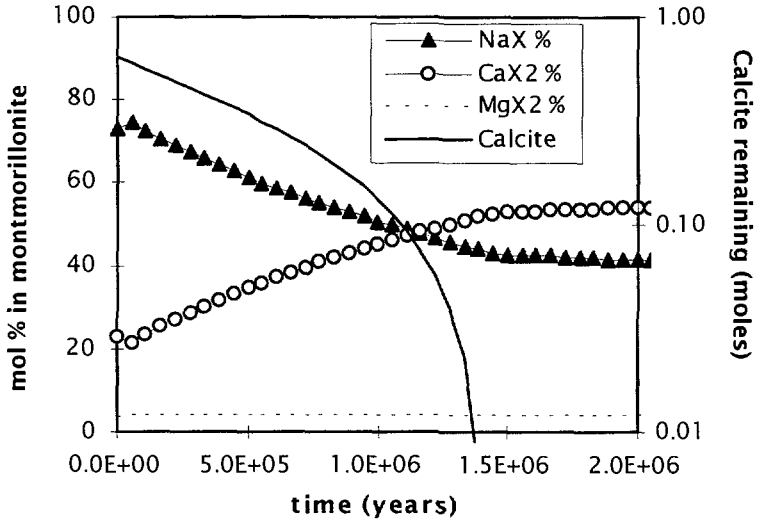

Figure 9-4.(cont.)

9.2.2 Effect of MX-80 bentonite accessory minerals on the buffer capacities

9.2.2.1 The effect of pyrite on the reducing capacity

The redox buffer exerted by pyrite is illustrated in Figure 9-5, where the change in pe due to the total pyrite dissolution is simulated, using different pyrite contents and oxygen fugacities.

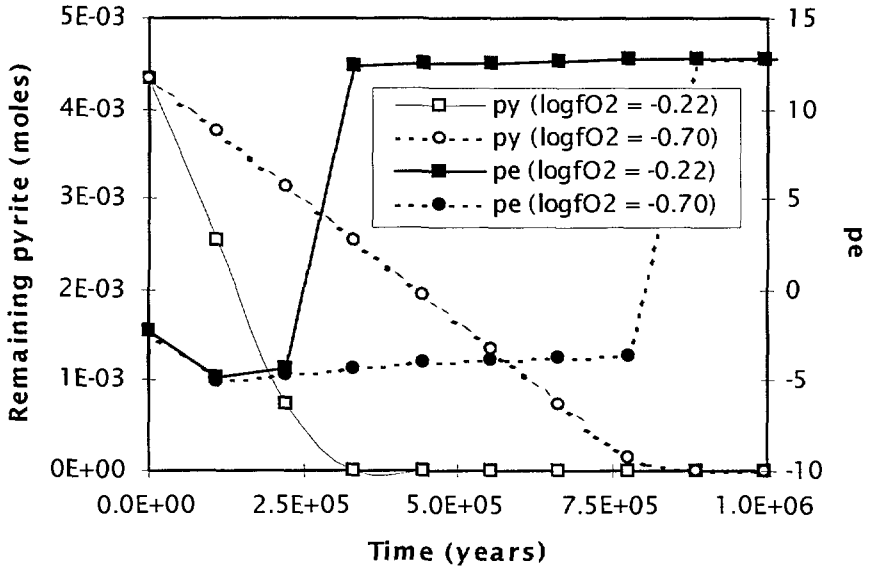

Figure 9-5. *Effect of the total pyrite dissolution on the redox state of the system (py: remaining pyrite). Äspö groundwater.*

From the previous results it seems clear that pyrite effectively prevents the oxidant intrusion in the system for a few thousand years even when unrealistically high oxygen fugacities are assumed.

On the other hand, if we assumed that the intruding groundwaters have been already exposed to the reducing capacity of the host rock, and their reflect their undisturbed reducing redox state, the reducing capacity of the bentonite system will not be affected.

9.2.2.2 The effect of calcite on buffering the alkalinity of the system

As we have previously discussed and in the light of the time evolution calculations, it is clear that calcite constitutes the main alkalinity buffering component of the bentonite system. In Figure 9-6, we explore the time required to deplete this buffering capacity when exposed to Finnsjön groundwaters. The results of this calculations indicate that, quite independently from the redox condition of the intruding groundwater, the alkalinity buffer is active for a million years period.

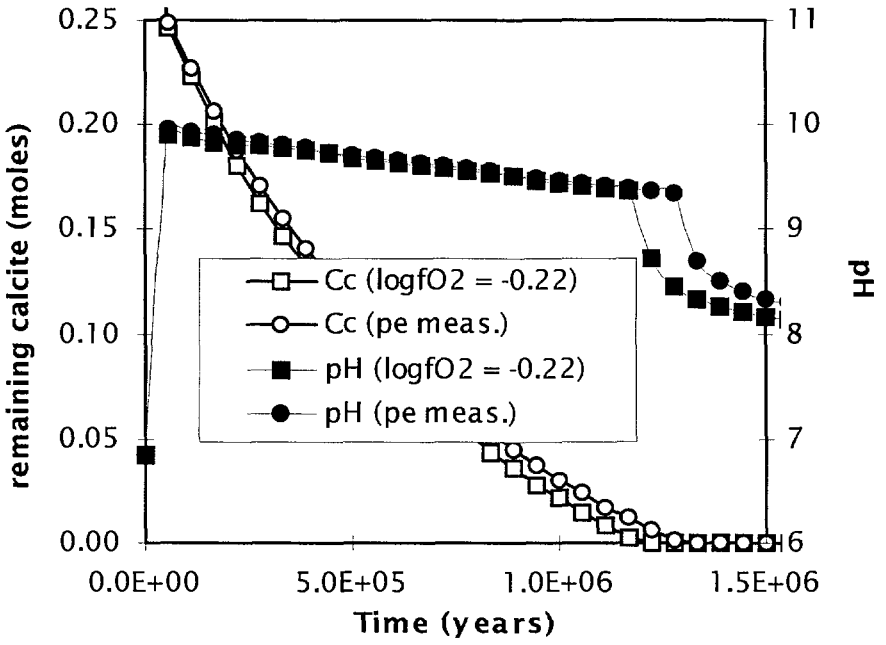

Figure 9-6. *Effect of the total calcite dissolution on the pH of the system (Cc: remaining calcite). Finnsjön groundwater.*

9.3 Spatial and time evolution of the bentonite-groundwater system

In these set of calculations we have attempted to investigate the spatial and time dependent effects on the chemical evolution of the bentonite buffer. The physical system has been devised as follows:

The 3.5 dm thick bentonite buffer is divided into five cells (each 0.7 dm thick), perpendicular to the groundwater flow direction. The water flow has been assumed in a conservative fashion to be: $Q_{eq} = 2 \cdot 10^{-3}$ m^3/year, which is 10 times faster than in previous time evolution calculations and assumes a replacement time for water in the bentonite of 1,000 years.

In the simulation new groundwater replaces porewater in the first cell, whereas the porewater of this cell replaces that of the next cell and so on, up to 500 replacements in each cell. This is equivalent to an evolution time of about 300,000 years.

For these calculations we have only used two groundwaters, Äspö and Gideå. However they should cover the span of chemical variability of Swedish granitic groundwaters.

Two different redox conditions have been assumed in the calculations: groundwaters in equilibrium with atmospheric oxygen (post-closure situation) and a 50/50 mix of the groundwaters with ice melting water with a composition is the result of previous calculations on the effect of oxygen intrusion in the redox stability at the disposal site (Guimerà et al, 1998).

The time-space evolution of the system for the two groundwater systems considered is presented in the following Figures. The results are presented in two different time-scales. Plots of the chemical and mineralogical evolution of the system in the initial 10,000 years are shown at the left side of the diagrams while the evolution up to 300,000 years is illustrated in the contour plots at the right side of the Figures.

9.3.1 Äspö, and Gideå groundwaters

9.3.1.1 Evolution of pH and Eh master variables

The results from Figures 9-7 to 9-9 could indicate that the alkalinity buffer capacity of the buffer material is initially depleted. This is the result of one of the critical assumptions of the calculations: we assume that the bentonite buffer is saturated with deionised water at the emplacement in the repository . Again, this is a result of the initial conditions of the calculations and it should not represent the behaviour of the buffer after emplacement. As the groundwater front moves into the buffer, the deionised water is pushed forward and consequently the dissolution of the accessory minerals occur, calcite in particular. In the longer term the alkalinity of the bentonite system

is restored. If we do not assume this initial deionised water saturation of the buffer no major changes on the alkalinity of the pore water system may be observed. This should be more representative of the post-closure behaviour of the material. However, we feel that these results have some implications for repository design and particularly for bentonite saturation strategies and they should be analysed more carefully.

In terms of redox stability it is clear that if we assume that pyrite oxidation proceeds according to equilibrium the redox stability is ensured for the overall space and time span of the buffer material.

9.3.1.2 Mineralogical evolution

The general pattern in the four cases considered is the exchange of Na by Ca in the montmorillonite. This exchange is faster and more complete in the case of Äspö groundwater due to its larger Ca content. The dilution with ice melting water retards this exchange process.

As we have already discussed calcite is partially depleted (roughly 50% of the initial fraction) at the initial contact times through out the buffer due to the effect of the saturation with deionised water.

Only a 10% of the initial fraction of pyrite is consumed in order to ensure the redox buffering. Hence, 90% of the pyrite buffer capacity remains unused. This is a comfortable safety marginal which should cover potential processes and parameters affecting the role of pyrite as redox buffer, such as hypothetical kinetic controls on pyrite oxidation, effect of Fe(III) hydroxide coatings on pyrite due to oxidation, heterogeneity of the pyrite distribution in the bentonite buffer.

Moreover, we have also considered the role of another reducing capacity which is normally neglected in the case of bentonite. This is the existence of Fe(II) impurities in the carbonate accessory minerals. Calcite is documented to incorporate Fe(II) replacing Ca(II) and to more extent Mg(II) in carbonates (Deer et al, 1992). The miscibility of Fe(II) in these carbonates at low temperatures is in the range: 0.01 to 0.1. We have performed a sensitivity analysis of the potential redox buffering role of this Fe(II) content by assuming a 0.013 molar fraction of siderite ($FeCO_3$) in the 1.4 wt. % of calcite reported in the bentonite. In this case no pyrite is assumed to be present in the buffer. When this siderite containing bentonite is exposed to Äspö groundwater, the system is kept basically reducing. Only the effect of deionised water in the saturation of the buffer material has a potential effect (see Figure 9-2). Again this is an hypothesis worth exploring and it would be interesting to analyse the amount of Fe(II) present in the calcite content of MX-80 bentonite. Such a characterisation has not been made as far as we are aware.

Äspö

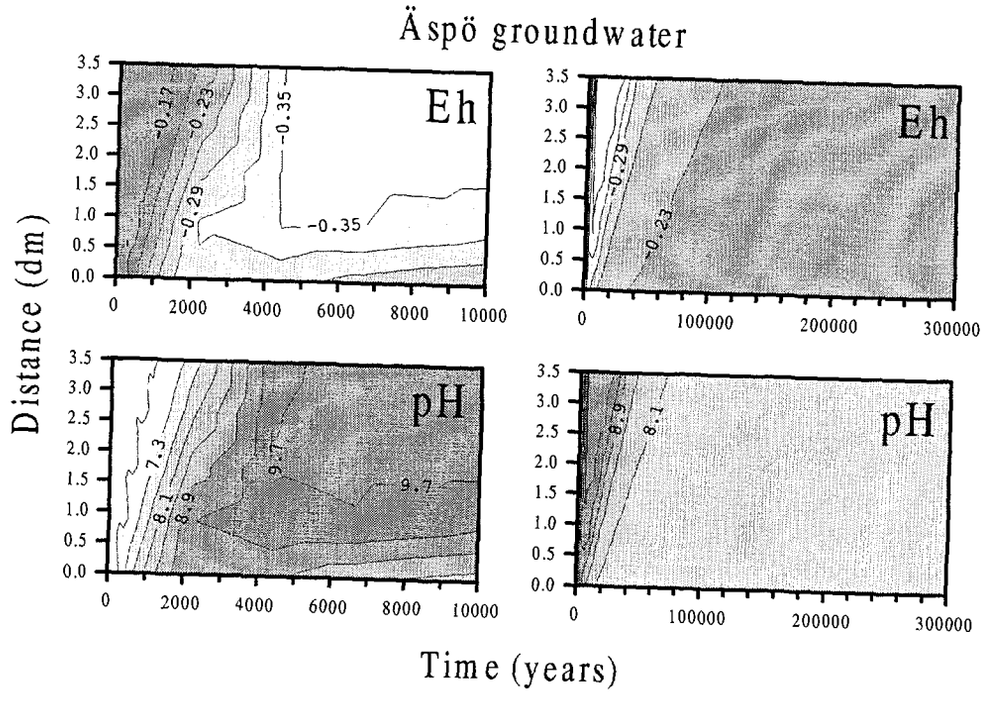
Äspö groundwater
Eh
pH
Distance (dm)
Time (years)

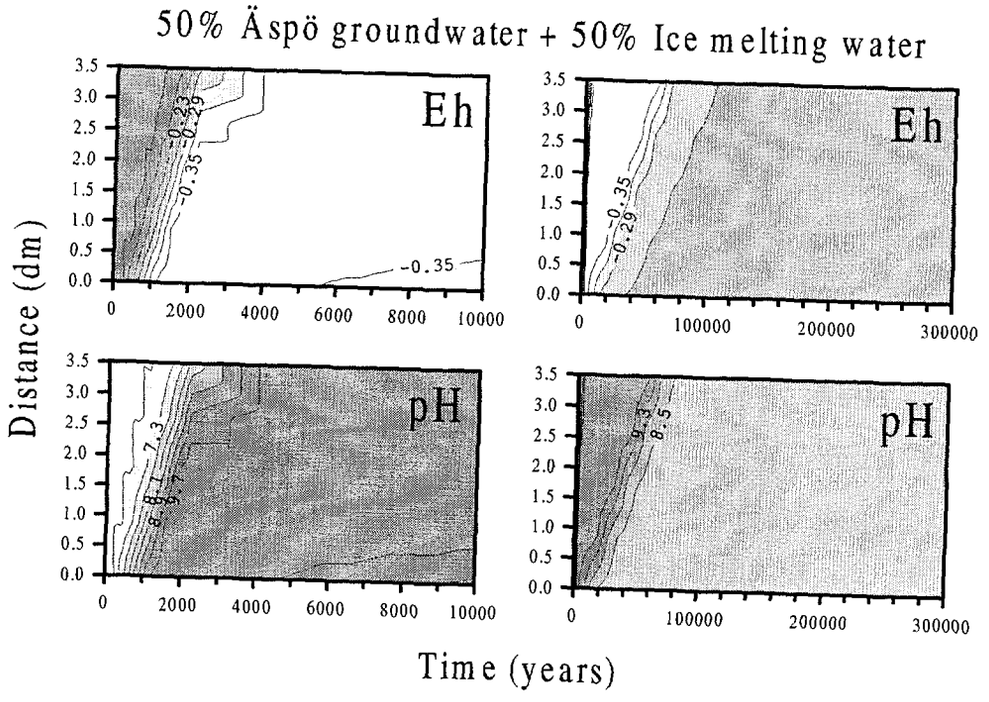
50% Äspö groundwater + 50% Ice melting water
Eh
pH
Distance (dm)
Time (years)

Äspö

Äspö groundwater

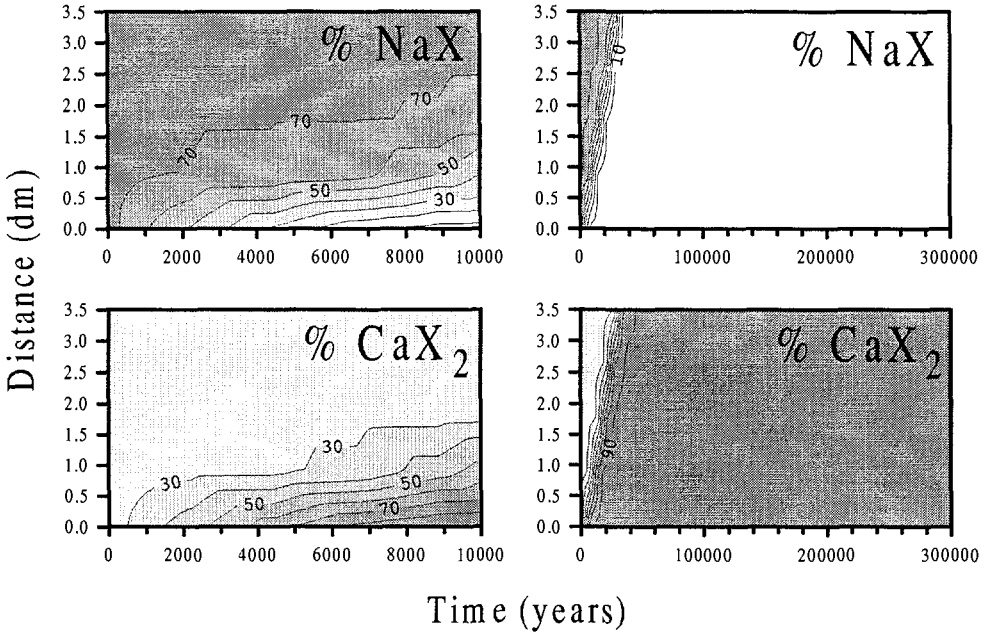

50% Äspö groundwater + 50% Ice melting water

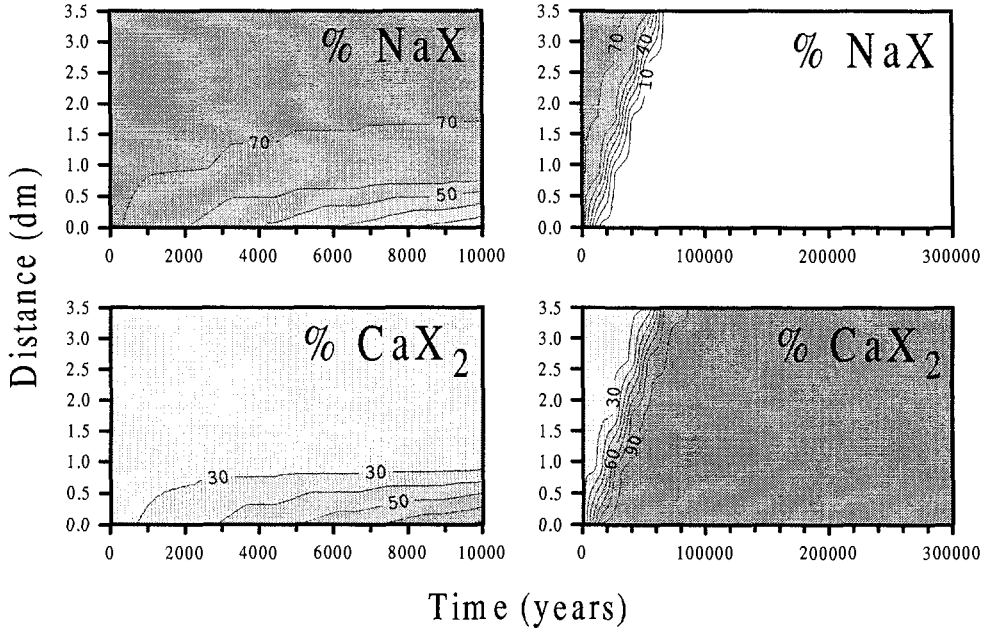

Äspö

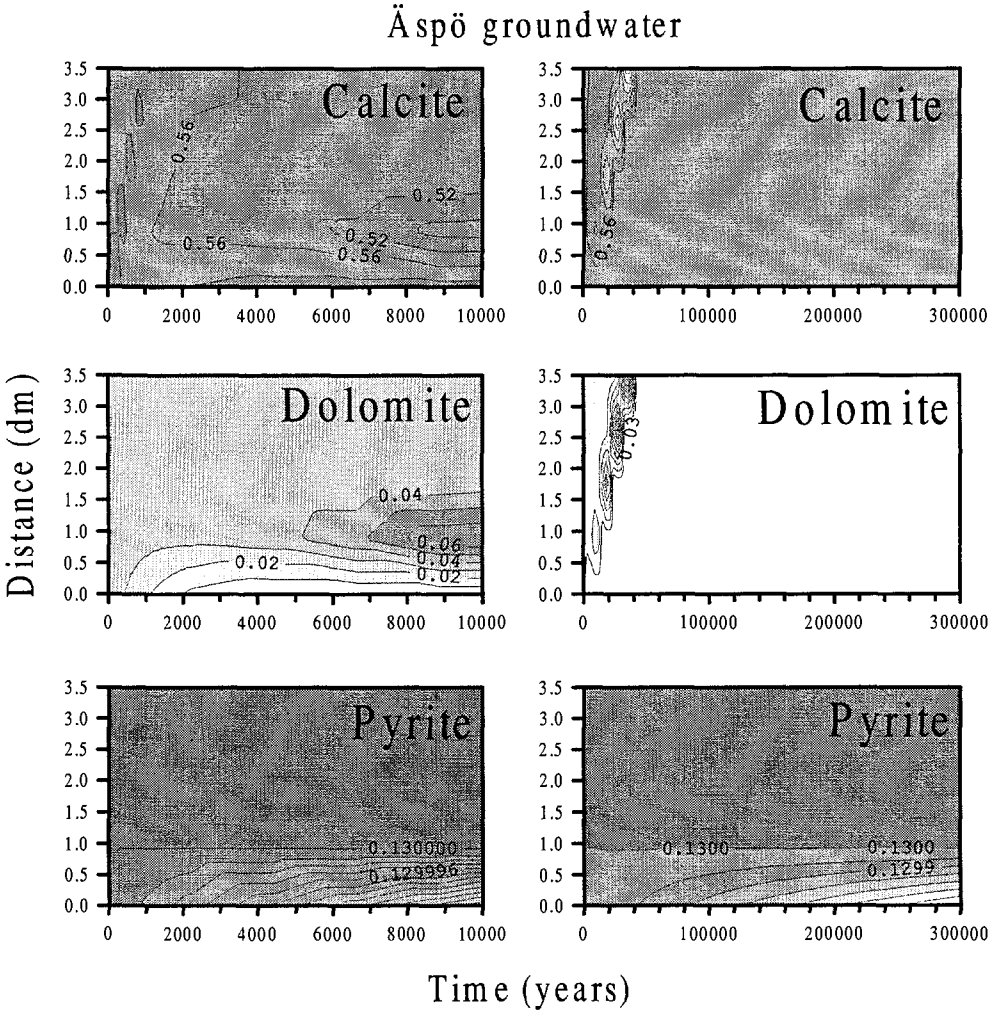
Äspö groundwater
Calcite
Calcite
Dolomite
Dolomite
Pyrite
Pyrite
Distance (dm)
Time (years)
0.56
0.52
0.04
0.06
0.02
0.03
0.130000
0.129996
0.1300
0.1299
0
2000
4000
6000
8000
10000
100000
200000
300000
0.0
0.5
1.0
1.5
2.0
2.5
3.0
3.5

Äspö

50% Äspö groundwater + 50% Ice melting water

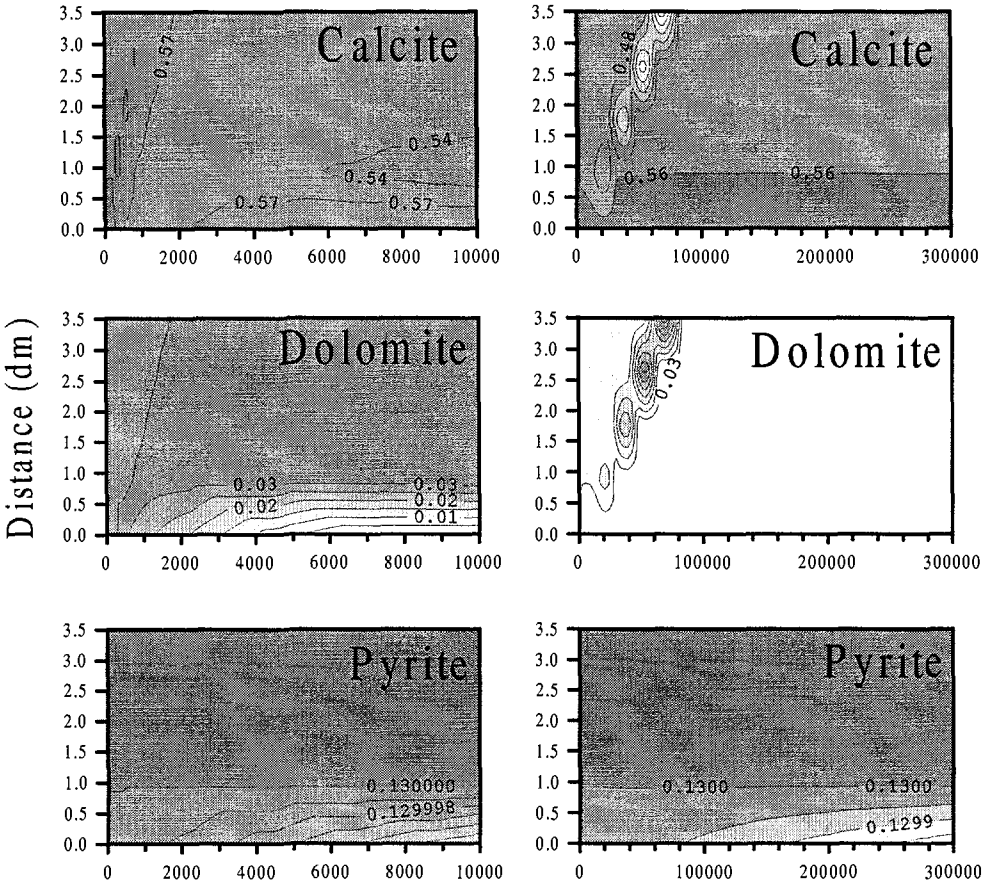

Gideå

Gideå groundwater

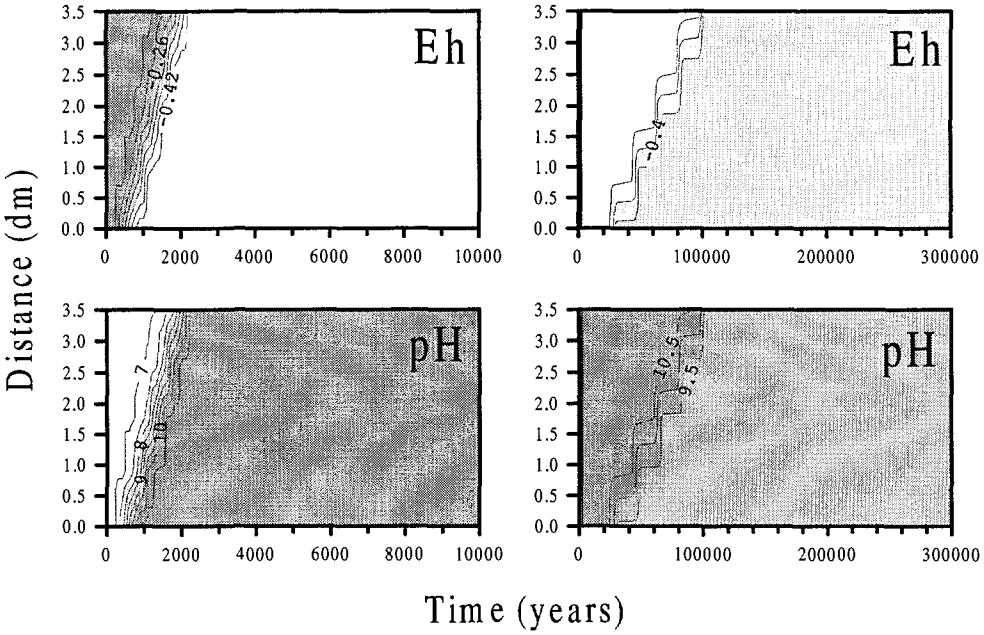

50% Gideå groundwater + 50% Ice melting water

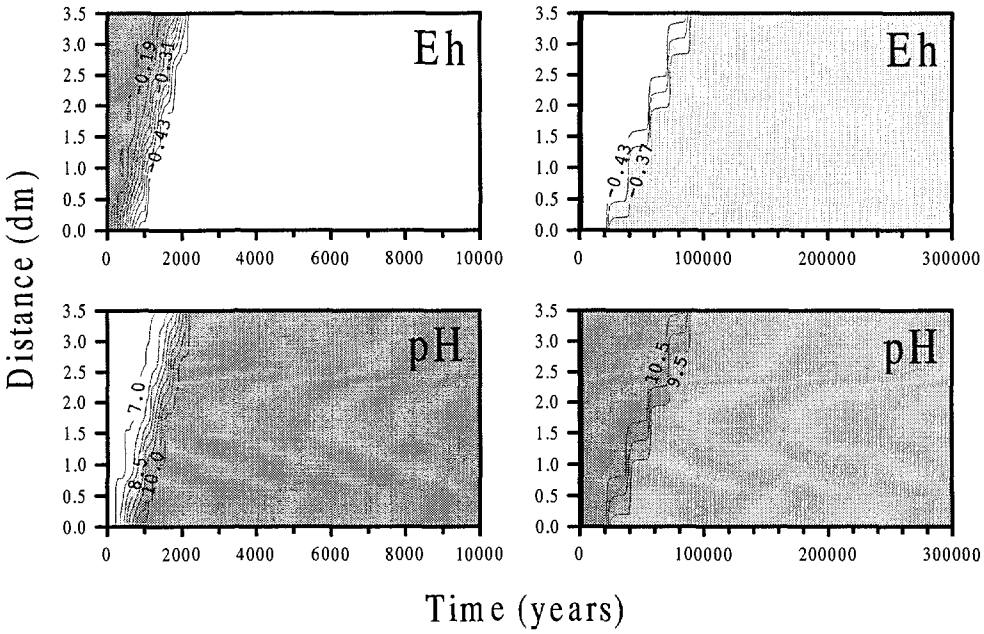

Gideå

Gideå groundwater

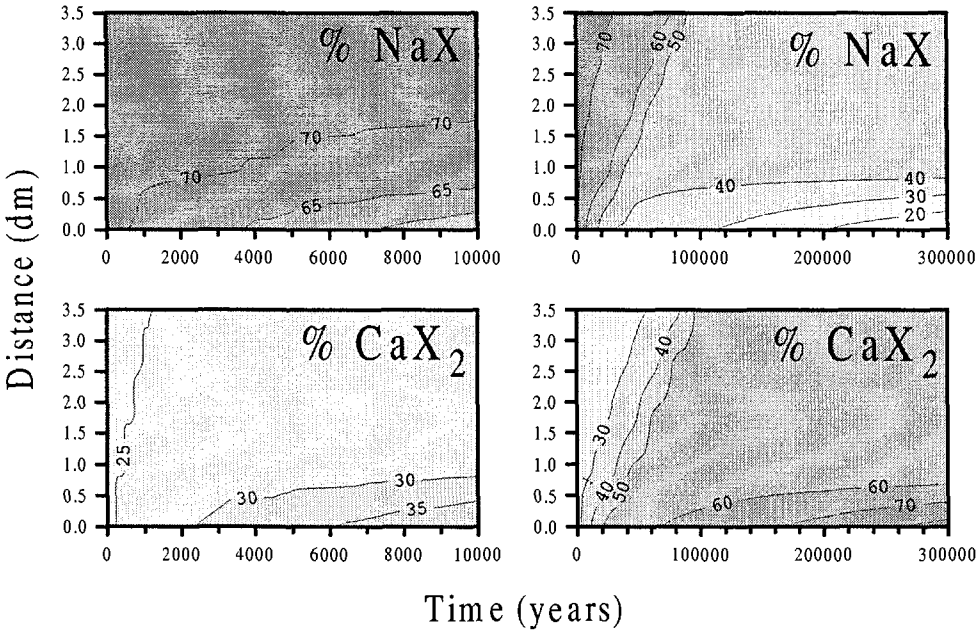

50% Gideå groundwater + 50% Ice melting water

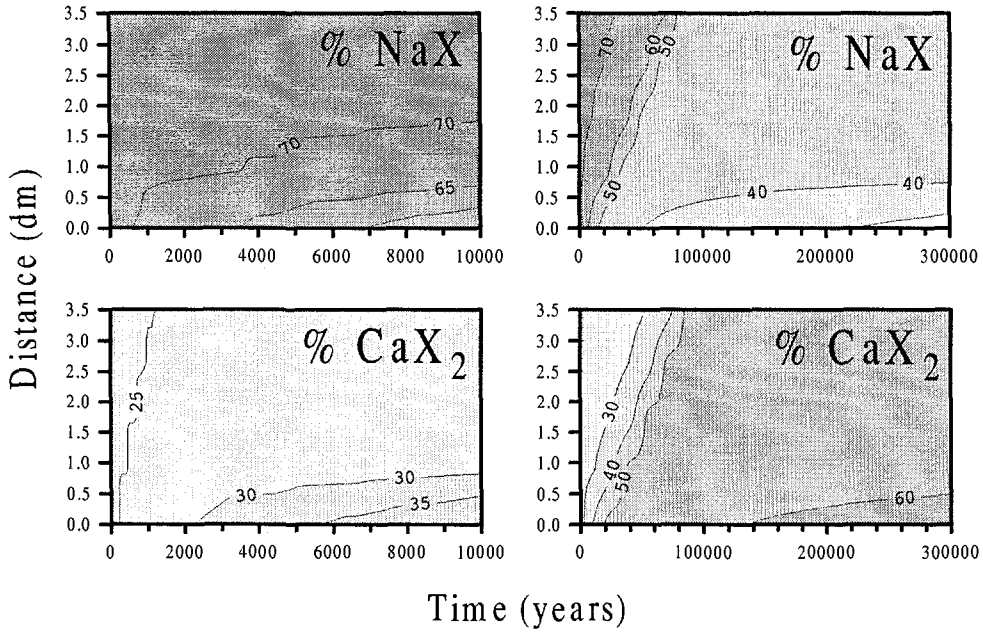

Gideå

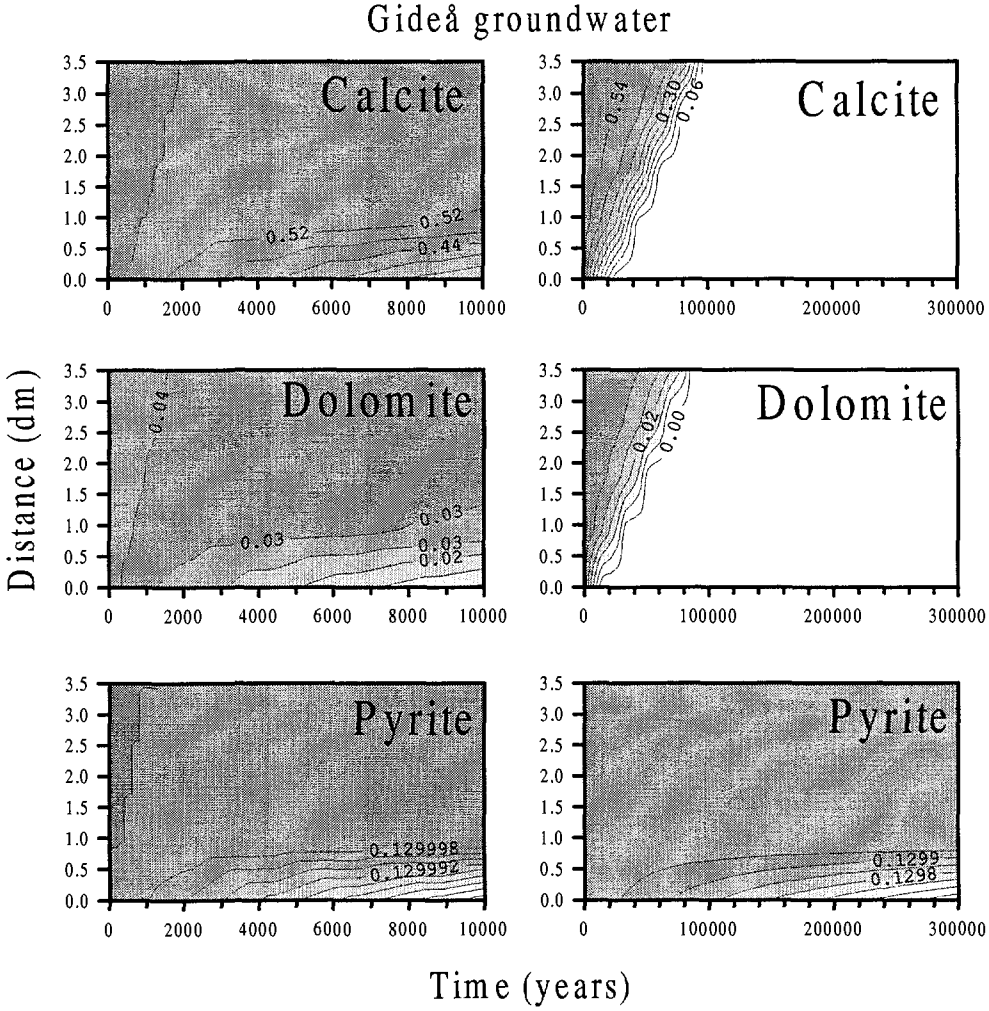
Gideå groundwater
Calcite
Calcite
Dolomite
Dolomite
Pyrite
Pyrite
Distance (dm)
Time (years)

Gideå

50% Gideå groundwater + 50% Ice melting water

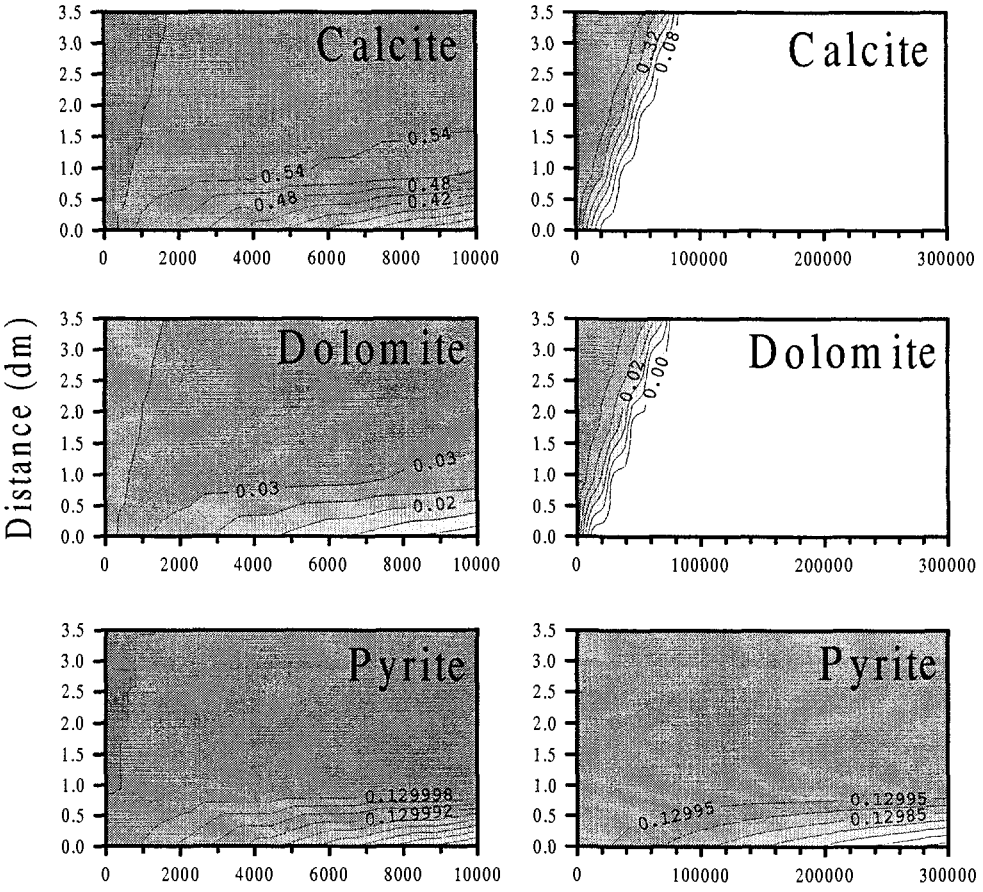

Äspö

$X^{sid}_{carb}=0.013$

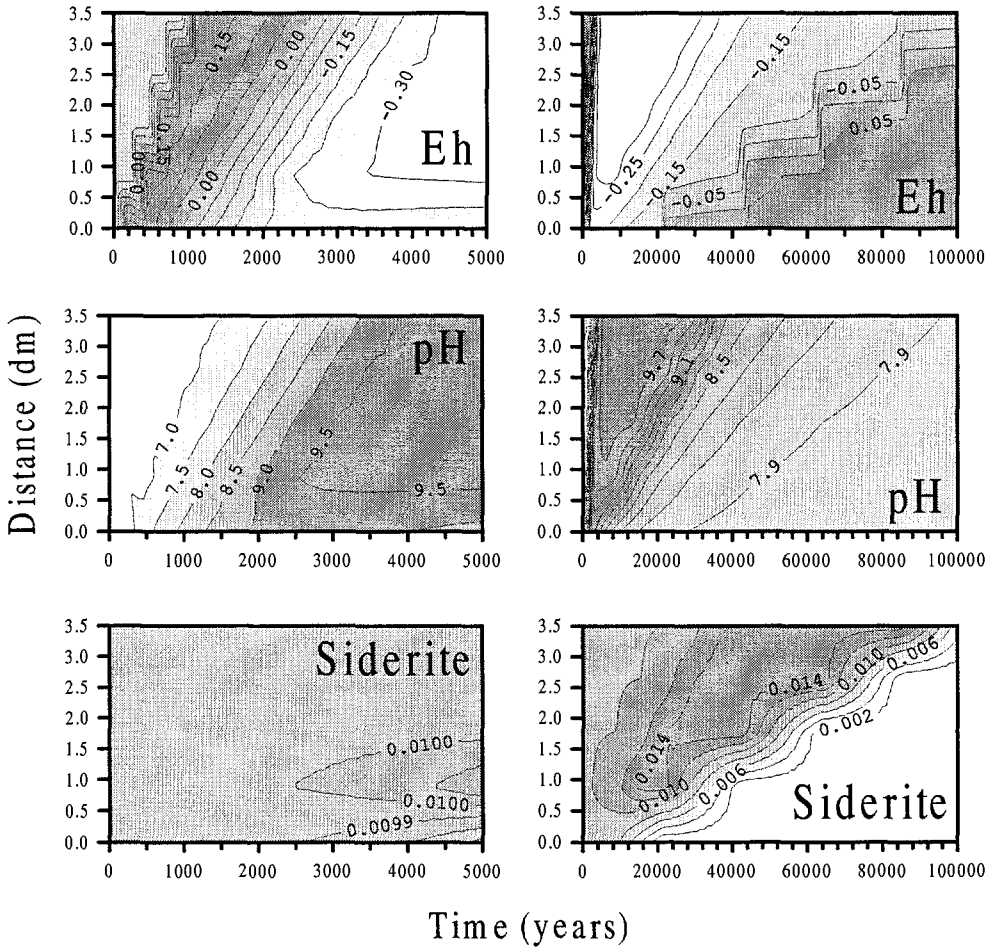

NEXT PAGE(S) left BLANK

10 Conclusions

The main processes affecting the chemical stability of the bentonite porewater system are:

- alkalinity buffering mainly due to calcite dissolution and precipitation and H^+ exchange reactions at the montmorillonite surface.

- redox buffering mainly due to the oxidation of pyrite and other Fe(II) accessory minerals contained in the bentonite.

These chemical buffering capacities are not largely affected by the replacement of porewater with granitic groundwater, either from Äspö, Gideå or Finnsjön. The main disturbance for the pH buffering capacity arises from the pre-saturation of the bentonite buffer with deionised water. The consequences of this into repository design and particularly bentonite saturation strategies should be analysed. Current full scale tests being performed at Äspö Hard Rock Laboratory should bring some additional light into this matter.

The redox buffer capacity exerted by the pyrite impurity is comfortably large. In the case when oxic waters are in contact with the buffer only some 10% of the reducing capacity exerted by the pyrite content is used. Additional and more labile reducing capacity could be given by the potential Fe(II) impurity content of the calcium and magnesium carbonates present in MX-80 montmorillonite.

References

Ahlbom K and Smellie J A T, 1989. Characterization of fracture zone 2, Finnsjön study site. SKB TR 89-19.

Bäckblom G, 1996. Preliminär utformning av djupförvarets närområde, SKB AR D-96-011

Deer W A, Howie R A and Zussman J, 1992. An Introduction to Rock Forming Minerals Longman Scientific and Technical, p. 626-27.

Fritz B and Kam M, 1985. Chemical interactions between the bentonite and the natural solutions from the granite near a repository for spent nuclear fuel. SKB TR 85-10.

Grenthe I, Stumm W, Laaksuharju M, Nilsson A C and Wikberg P, 1992. Redox potentials and redox reactions in deep groundwater systems. Chemical Geology 98, 131-150.

Lajudie A, Raynal J, Petit J C and Toulhoat P, 1995. -Clay based materials for engineered barriers: a review. MRS Symp. Proc., 353, 221-230.

Laurent S, 1983. Analysis of groundwater from deep boreholes in Gideå. SKBF, SKB TR 83-17.

McKinley I G, 1984. The geochemistry of the near field, Nagra NTB 84-48, Baden, Switzerland.

Müller-Vonmoos M and Kahr G, 1985. Langzeitverhalten von Bentonit under endlagerbedingungen. Nagra NTB 85-25, Baden, Switzerland.

Olin M, Lehikoinen J and Muurinen A, 1995. MRS Symp. Proc., 353, 253-260.

Parkhurst D L, 1995. User's guide to phreeqc- a computer program for speciation, reaction-path, advective-transport, and inverse geochemical calculations. USGS. Water-resources investigations report 95-4227. 143 pp.

Sasaki Y, Shibata M, Yui M and Ishikawa H, 1995. Experimental studies on the interaction of groundwater with bentonite. MRS Symp. Proc., 353, 337-344.

SKI SITE-94, 1996. SKI Site 94 Deep Repository performance assessment projects. SKI Report 96:36.

SR 95, 1996. Template for safety reports with descriptive example. SKB TR 96-05.

Van Olphen H and Fripiat J J, 1979. Data handbook for clay minerals and other non-metallic minerals. Pergamon Press. New York, 346 pp.

Wanner H, Wersin P and Sierro N, 1992. Thermodynamic modelling of bentonite-groundwater interaction and implications for near field chemistry in a repository for spent fuel. SKB TR 92-37.

Wieland E, Wanner H, Albinsson Y, Wersin P and Karnland O, 1994. A surface chemical model lof the bentonite-water interface and its implications for modelling the near field chemistry in a repository for spent fuel. SKB TR 94-26.